Journal of Photochemistry & Photobiology, B: Biology 234 (2022) 112549

Contents lists available at ScienceDirect

Journal of Photochemistry & Photobiology, B: Biology

journal homepage: www.elsevier.com/locate/jphotobiol

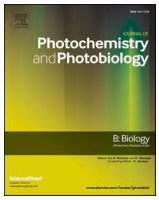

Fast chlorophyll *a* fluorescence induction (OJIP) phenotyping of chlorophyll-deficient wheat suggests that an enlarged acceptor pool size of Photosystem I helps compensate for a deregulated photosynthetic electron flow

Lorenzo Ferroni [a,b,*], Marek Živčak [b], Marek Kovar [b], Andrea Colpo [a], Simonetta Pancaldi [a], Suleyman I. Allakhverdiev [c], Marian Brestič [b,**]

[a] Laboratory of Plant Cytophysiology, Department of Environmental and Prevention Sciences, University of Ferrara, Ferrara, Italy
[b] Department of Plant Physiology, Slovak University of Agriculture, Nitra, Slovakia
[c] K.A. Timiryazev Institute of Plant Physiology, RAS, Botanicheskaya Street 35, Moscow 127276, Russia

ARTICLE INFO

Keywords:
Chlorophyll-deficient wheat
Prompt chlorophyll fluorescence
Electron transport
Fluctuating light
Photosynthesis phenotyping

ABSTRACT

The wheat lines affected by a decrease in the leaf chlorophyll content typically experience a biomass loss. A known major problem of the chlorophyll-deficient wheat mutants is their limited prevention of Photosystem I (PSI) over-reduction brought about by an insufficient cyclic electron flow, potentially exposing them to a higher sensitivity to light fluctuations. However, the resistance of some mutant lines against fluctuating light suggests the occurrence of regulatory processes compensating for the defect in cyclic electron flow. In this study, a phenotyping approach based on fast chlorophyll *a* fluorescence induction (OJIP transient), corroborated by P700 redox kinetics, was applied to a collection of chlorophyll-deficient wheat lines, grown under continuous or fluctuating light. Quantitative parameters calculated from the OJIP transient are considered informative about Photosystem II (PSII) functional antenna size and photochemistry, as well as the functioning of the entire photosynthetic electron transport chain. The mutants tended to recover a wild-type-like chlorophyll content, and mature plants could hardly be distinguished based on their effective PSII antenna size. Nevertheless, specific OJIP-derived parameters were strongly correlated with the phenotype severity, in particular the amplitude of the I-P phase and the I-P/J-P amplitude ratio, which are indicative of a more capacitive pool of PSI final electron acceptors (ferredoxin and ferredoxin-$NADP^+$ oxidoreductase, FNR). We propose that the enlargement of such pool of electron carriers is a compensatory response operating at the acceptor side of PSI to alleviate potentially harmful over-reduced states of PSI. Our results also suggest that, in chlorophyll-deficient mutants, higher F_V/F_M cannot prove a superior PSII photochemistry and wider I-P phase is not indicative of a higher relative content of PSI.

1. Introduction

The response of plant photosynthesis to natural light fluctuations is a current hot topic in plant biology, with special regard to crops and their productivity [47,69,77]. Information is still fragmentary but indicates the importance of a proper regulation of the photosynthetic electron transport from photosystem II (PSII) to photosystem I (PSI) and its final downstream acceptors, primarily the carbon fixation reactions. A sudden rise in irradiance challenges the regulation of the photosynthetic electron flow because it causes a strong inflow of electrons from PSII into the transport chain, leading to a temporary over-reduction at the PSI donor side [88]. The potential consequence of repetitive excessive light absorption and reducing bursts is the photodamage of PSII and PSI, the latter being particularly sensitive to over-reduced states [22,30,65]. The safe thermal dissipation of excess absorbed energy (non-photochemical quenching of chlorophyll fluorescence, NPQ), the activation of cyclic electron flow (CEF), the regulation of the energy distribution between PSI and PSII, and the exploitation of electron sinks alternative to

* Corresponding author at: Department of Environmental and Prevention Sciences, University of Ferrara, Ferrara, Italy.
** Corresponding author at: Department of Plant Physiology, Slovak University of Agriculture, Nitra, Slovakia.
E-mail addresses: lorenzo.ferroni@unife.it (L. Ferroni), marian.brestic@uniag.sk (M. Brestič).

https://doi.org/10.1016/j.jphotobiol.2022.112549
Received 31 August 2021; Received in revised form 10 August 2022; Accepted 16 August 2022
Available online 19 August 2022

photosynthesis and photorespiration are the main mechanisms that limit the potential damage caused by reducing bursts, particularly enabling the safe accumulation of oxidised PSI complexes [23,65,74–76,80,81,87]. Long-term acclimation of plants to a fluctuating light (FL) regime is expected to enhance such protective mechanisms.

Acclimation of plants to a FL regime leads to special properties of the photosynthetic membrane, which are not exactly intermediate between the well-characterized properties of sun- or shade-acclimated plants [1,46]. The thylakoid membrane of FL plants rather combines some characteristics of the former and the latter, but it also develops additional unique properties, which altogether enable a superior flexibility [36,67,88]. In *Arabidopsis thaliana*, the long-term acclimation to light-flecks was reported to lead to a lower chlorophyll *a/b* ratio, indicating a tendency to increase the light harvesting capacity ([47,67] and references therein). Nevertheless, this inference could be not valid in other species [35,55] and even in Arabidopsis a comprehensive transcriptomic analysis revealed instead a generalized downregulation of LHCB proteins of the PSII antenna system [63]. A lower light-harvesting capacity, due to a smaller PSII functional antenna size, can conceivably be beneficial to reduce the excitation pressure on PSII, while the parallel upregulation of NPQ and CEF under FL limits the electron pressure on PSI [49,55,63]. Therefore, the logical conclusion would be that a successful acclimation to a FL regime could benefit from a small PSII antenna size, but only if it is coupled with the effective thylakoid regulation that favours the electron outflow from PSI.

Chlorophyll-deficient (*chlorina*) wheat lines represent an interesting biological material in this respect. Analysis of *chlorina* mutants has a long history in studies aimed at clarifying chlorophyll metabolism, photosynthetic physiology and thylakoid organization in crops and other model plants (e.g., [14,19,78]). A genetic lesion affecting the magnesium chelatase causes a decrease in the leaf chlorophyll content, especially chlorophyll *b*, and results in an untargeted antennae downsizing [14,31,32,92]. The retarded growth of *chlorina* mutants is thought to be mainly the consequence of an altered dynamic regulation of photosynthetic electron flow because of imbalanced excitation rates of PSI and PSII [2,79]. A biochemical feature repeatedly reported is a lower PSI/PSII reaction centre ratio [2,6,19,21,78]. In order to explore a possible agricultural use, the mutated genes in typical *chlorina* wheat mutants were introduced into vigorous genotypes by crossing, leading to the selection of near-isogenic *chlorina* mutants *sensu lato* [90]. Depending on the genomic context and the mutated locus, such chlorophyll-deficient wheat lines differ greatly with respect to the severity of their yellow-green phenotype. A collection of six chlorophyll-deficient wheat lines analysed under controlled conditions have a typically lower leaf chlorophyll content at early stages of growth and subsequently tend to recover a WT-like phenotype ([98]; Table 1). Compared to the WT NS67, the chlorophyll *a/b* ratio is higher in ANK32A, but not in the lines ANBW4A and ANBW4B. Durum wheat lines ANDW7A, ANDW8A, ANDW7B have a higher chlorophyll *a/b* ratio especially at early growth stages in comparison with the WT LD222 ([98]; Table 1). Mature ANDW7A and ANDW7B share a reduced chlorophyll content by ca. 35%, but only the latter maintains a significantly higher chlorophyll *a/b* ratio (Table 1). Therefore, the relation between chlorophyll content and PSII antenna size seems to weaken during the plant growth. Growth under outdoor conditions showed that even a slightly lower concentration of leaf chlorophyll was not an innocent variation but had a negative impact on the plant performance [98]. A major problem of the mutants was their limited prevention of PSI over-reduction brought about by an insufficient CEF [98]. Because the detrimental consequences of the lesion could be enhanced by the repetitive exposure to highlight flecks, the same mutants were then analysed comparatively under a FL or a continuous light regime (CL) during a broad-scope phenotyping experiment carried out at the Slovak PlantScreen™ Phenotyping Unit (SPPU) [15]. In Table 1, the mutants have been ordered by increasing severity based on their biomass accumulation under CL [15]. Importantly, the

Table 1
Severity of the chlorophyll-deficient wheat lines used in this phenotyping study in comparison with their wild-type lines (NS67, LD222). The values of chlorophyll content and chlorophyll *a/b* ratio are those reported by Živčak et al. [98] and measured under standard growth chamber conditions. The values of aboveground biomass of the same mutants grown under a continuous (CL) or fluctuating (FL) light regime are those obtained by Ferroni et al. [15], here expressed as percentage of the wild-type lines under CL. Conditional cell formatting shows increasing severity of biomass depletion with darker colour.

Bread wheat

		NS67	**ANBW4B**	**ANBW4A**	**ANK32A**
Mutated locus		Wild-type	*cnB1-d*	*cnA1-d*	*cnA1-a*
Chlorophyll content ($g\ m^{-2}$)	Young	0.35	0.18	0.20	0.11
	Mature	0.56	0.57	0.51	0.38
Chlorophyll *a/b*	Young	2.3	2.0	2.0	4.7
	Mature	2.9	2.6	3.1	4.0
Biomass yield in Light regime	**CL**	100%	91%	75%	54%
	FL	86%	57%	102%	52%

Durum wheat

		LD222	**ANDW7A**	**ANDW8A**	**ANDW7B**
Mutated locus		Wild-type	*cnA1-d*	unknown	*cnB1-d*
Chlorophyll content ($g\ m^{-2}$)	Young	0.28	0.11	0.15	0.10
	Mature	0.45	0.28	0.42	0.30
Chlorophyll *a/b*	Young	2.5	4.1	3.2	5.1
	Mature	2.9	3.2	3.5	3.7
Biomass yield in Light regime	**CL**	100%	75%	75%	57%
	FL	89%	69%	72%	39%

long-term response of the mutants to FL did not confirm the anticipated principle "the stronger the chlorophyll depletion, the worse the resistance to FL". Only ANBW4B and ANDW7B were strongly compromised by FL, while the others behaved almost the same, including the severely impaired mutant ANK32A, which is affected the most in CEF [6,7,15,98]. In ANK32A, we could not find evidence for the induction of a compensatory electron flow downstream of PSI, such as an increased electron sink capacity of the Calvin-Benson-Bassham cycle or alternative electron flows [15]. To solve the enigmatic resistance of some chlorophyll-deficient mutants against FL, other potential regulatory processes may be hypothesized, such as adjustments in the intersystem electron transport chain.

During the experiment at the SPPU, the chlorophyll-deficient mutant lines were also monitored using direct chlorophyll *a* fluorescence emission. This fast and non-invasive measurement, conducted with a portable HandyPEA instrument, responds to two important requirements in plant phenotyping research: (a) causing negligible perturbations to the plant and (b) allowing the accumulation of many measurements in a short time [27]. Accordingly, a fast fluorescence-based dynamic phenotyping can take into account mutation-, treatment- and age-related variations. In the planning phase of our experiment, its main scope was to ascertain whether under FL the mutants underwent PSII photoinhibition; however, the prompt PSII fluorescence transient – called OJIP – is very rich in information and can also prove, or not, the occurrence of adjustments of the intersystem electron transport chain in the mutants. The transient is recorded from a dark-acclimated sample exposed to a saturating light pulse. The emitted chlorophyll fluorescence has a very typical trace, usually shown on a logarithmic timescale: from the minimal value (F_0) at the initial step O, it increases up to a maximum value (F_M) at step P (Fig. 1). The F_0-F_M difference is the variable fluorescence of PSII (F_V). Two inflections, termed steps J and I, occur between O and P, at ca. 2 and 30 ms from O. The fast O-J phase is termed "photochemical", the subsequent slower J-I-P rise is known as the "thermal" phase [71]. For decades, the analysis of the OJIP transient has represented a powerful tool to investigate the photosynthetic physiology, in particular PSII functional antenna size, PSII photochemistry, redox state of the photosynthetic electron transport chain and PSI/PSII stoichiometry (see for review e.g., [25,27,70]).

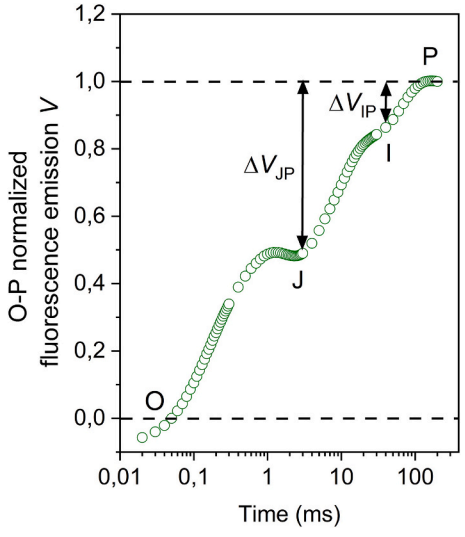

Fig. 1. Example of a fast chlorophyll *a* fluorescence transient in the wild-type bread wheat NS67. The transient was recorded under the conditions described in the main text, Section 2.2. The transient was double normalized between steps O sampled at 50 μs and P, generally reached around 200 ms. O-P double-normalized fluorescence emission is indicated as *V*. The intermediate steps J and I are shown, sampled at 2 and 30 ms, respectively. The complement to 1 of the relative fluorescence at step J (ΔV_{JP}) and I (ΔV_{IP}) are indicated.

Moreover, it is an elective analytical tool for the phenotyping of crop accessions/mutants in response to stresses (see for review [26,72]). Particularly popular has become the so-called "JIP-test", which characterizes the OJIP transient by means of many biophysical parameters, quantum yields and probabilities derived from the *theory of the energy fluxes* [70,73]. The test relies on the conventional understanding of the F_V origin according to the "Q_A model" of Duysens and Sweers [13], which is widely accepted as a good approximation [84]. Nevertheless, the validity of the Q_A model continues to be a hotly debated topic [62,68,71,86], which however is beyond the scope of our phenotyping experiment. Importantly, and not necessarily interpreted within a pure Q_A model, some JIP parameters describe basic geometrical properties of the OJIP transient that can be related to certain functional aspects with a good degree of confidence. Calculated from massive data sets, they can allow the mining of *regularities* through wheat samples with a variable extent of chlorophyll depletion.

2. Material and Methods

2.1. Plant Material and Experimental Design

The plant material used in this report is the same described in detail by Ferroni et al. [15] for the "TriPUDIUM" phenotyping experiment conducted in the frame of the European Plant Phenotyping Network 2020 (EPPN^{2020}). Eight wheat lines were used: for bread wheat (*Triticum aestivum*), the chlorophyll-deficient lines were ANBW4A, ANBW4B, ANK32A, and the corresponding WT cv. Novosibirskaya 67, NS67; for durum wheat (*Triticum durum*), the chlorophyll-deficient lines were ANDW7A, ANDW7B, ANDW8A, and the corresponding WT, LD222. Their typical chlorophyll contents in growth chamber conditions are reported in Table 1. The experiment consisted of a strictly controlled cultivation that was set up at the SPPU (Agrobiotech Centre of the Slovak University of Agriculture in Nitra, Slovak Republic), where the plants were transferred after germination and distributed in two sectors differing only with respect to the light regime, CL or FL. In both cases, the light source was a cool white LED-bar system providing a daily light integral of ca. 16 mol photons m^{-2} day^{-1} during a photoperiod of 14 h (06:00–20:00 local time). Control of light intensity and the frequency of lightflecks was performed by Fytotron Light Control software (PSI, Drasov, CZ). In the CL sector, the irradiance gradually rose during the morning (06:00–11:00) up to a plateau of 500 μmol photons m^{-2} s^{-1} lasting for 4 h (11:00–15:00) and followed by a gradual decrease in the afternoon (15:00–20:00). In the FL sector, the parameters set up in Fytotron Light Control were as follows: Amplitude 60%; Cloud attenuation 0.20; Cloud density 90; Cloud duration mean 1.0; Cloud duration var. 50; Fluctuation var. 10; Fluctuation mean ratio 0.50. The resulting FL regime allowed the same average daily outline of irradiance as in the CL sector, but the daily light integral was obtained through random fluctuations between ca. 100 and 1000 μmol photons m^{-2} s^{-1}. The fluctuations occurred on a timescale of a few minutes; every hour the plants received 16 lightflecks, overall simulating cloudflecks during a moderately bright day. Other environmental details of the experiment in SPPU are reported in Ferroni et al. [15].

Plants were analysed weekly for prompt chlorophyll florescence emission during four subsequent weeks, starting from the 35th day after sowing, when the plants had developed the fourth leaf. For each line and light regime, 4–7 independent plants (one plant per pot) were available for the measurements. At the end of the experiment, the chlorophyll content was analysed in acetonic extracts according to Živčak et al. [98] and using the Lichtenthaler's [38] equations.

2.2. Measurement of the Fast Chlorophyll a Fluorescence

The prompt chlorophyll *a* fluorescence emitted upon exposure to a saturating pulse was measured using a HandyPEA portable fluorometer (Plant Efficiency Analyzer, Hansatech Instruments, King's Lynn, Norfolk,

UK). Fluorescence was measured on the adaxial surface of the middle part of the youngest fully developed leaf of all plants. In order to reveal differential PSII photoinhibitory effects due to the light regime, all plants were measured at 9:00–10:00 in the morning and again in the afternoon at 14:00–15:00. The automated randomization of pot positions, done every second day, ensured that the sequential order of measured plants was never the same week after week, as well as any systematic positioning effects were excluded for the same reason.

The measuring protocol was the "double hit method" applied according to Strasser [73] and Mathur et al. [45]. In particular, the leaf was dark acclimated for 15 min using the leaf clip of the instrument and then the fluorescence transient was induced by applying a first 1 s-long saturating pulse at 3500 μmol photons m^{-2} s^{-1}. The light source consisted of three light-emitting diodes (LEDs) integrated in the measuring head of the instrument and providing orange-red light at 650 nm. After a dark interval of 500 ms from the first pulse, the second pulse, with the same characteristics as the first, was applied to the leaf.

2.3. Characterization of the Fluorescence Induction Transients

The OJIP transients obtained from the first pulse were analysed using selected parameters of the JIP test according to Strasser et al. [73] and Stirbet and Govindjee [70]. For the phenotyping purpose, some approximations are an acceptable compromise in view of the large amount of data recorded. Therefore, for the massive analysis of transients, basic and derived parameters were extracted using the Biolyzer software (Fluoromatic Software, Geneva, Switzerland), which samples the fluorescence values at fixed time points of the transient.

For the comparative analysis of PSII activity and photoinhibition under CL or FL, the maximum photochemical quantum yield of PSII was approximated as F_V/F_M [18]. For higher precision in the comparison, the F_0 value used for calculation was that extrapolated back to time 0. Per definition, PSII photoinhibition is a sustained loss of PSII photochemical yield, *Y(qI)*, independent of the mechanism [11]. It was assumed that residual minor NPQ components with decay times ≥10 min contributed negligibly (for references on minor NPQ components, see [16,40]). *Y(qI)* was calculated as the difference between F_V/F_M in the morning and in the afternoon for every single plant:

$$Y(qI) = \left(\frac{F_V}{F_M}\right)_{morning} - \left(\frac{F_V}{F_M}\right)_{afternoon} \quad (1)$$

The double hit method was used to further characterize PSII photochemistry. When a second saturating pulse is applied 500 ms after the first one, a lower F_V/F_M is measured, mostly due to a higher F_0. The lost fraction of F_V/F_M is denoted B_O and calculated as:

$$B_O = \frac{\left[\left(\frac{F_V}{F_M}\right) - \left(\frac{F_V^*}{F_M^*}\right)\right]}{\left(\frac{F_V}{F_M}\right)} \quad (2)$$

where F_V is the variable fluorescence of PSII calculated from the first pulse and F_V* is the variable fluorescence of PSII calculated from the second pulse from newly measured basal F_0* and maximum F_M* fluorescence. B_O was compared between values recorded in the morning and in the afternoon:

$$\Delta B_O = (B_O)_{afternoon} - (B_O)_{morning} \quad (3)$$

Other parameters used to describe the OJIP transients were chosen from those calculated by Biolyzer. F_0 at O was extracted at 50 μs ($F_{50\mu s}$) for calculation of derived parameters. F_J was extracted at 2 ms (step J), F_I at 30 ms (step I). Upon O-P normalization, the relative fluorescence values at the two inflections J and I were calculated as:

$$V_J = \left(F_J - F_{50\mu s}\right)/\left(F_M - F_{50\mu s}\right) \quad (4)$$

$$V_I = \left(F_I - F_{50\mu s}\right)/\left(F_M - F_{50\mu s}\right) \quad (5)$$

Their complement to one is indicated as ΔV_{JP} (=1-V_J) and ΔV_{IP} (=1-V_I), respectively (Fig. 1).

The initial part of the O-J phase (50–300 μs) is characterized by the slope M_o. The normalization of M_o on the relative fluorescence V_J and the F_V/F_M ratio provides an estimate of the apparent antenna size of an active PSII [73]:

$$\frac{ABS}{RC} = \frac{M_O}{V_J \frac{F_V}{F_M}} = \frac{\frac{4\left(F_{300\mu s} - F_{50\mu s}\right)}{F_V}}{V_J \frac{F_V}{F_M}} \quad (6)$$

The Area is the geometrical parameter corresponding to the total complementary area comprised between the OJIP curve and F_M. Upon normalization on F_V, the resulting Sm = Area/F_V is considered proportional to the number of electron transporters per PSII-PSI chain unit.

2.4. Simultaneous Measurement of P700 Redox State and Chlorophyll Fluorescence

The simultaneous analysis of the fast chlorophyll *a* fluorescence induction and P700 redox state was performed with a Dual PAM-100 (Walz, Germany; [29,96]). Wheat plants sampled from the growth facility were dark acclimated for 15 min in a dark box and subsequently for ca. 2 min in the measuring head. The sample was then exposed to a 0.5 s-long saturation pulse (10.000 μmol photons m^{-2} s^{-1}), during which the chlorophyll fluorescence emission and the relative abundance of $P700^+$ were recorded simultaneously at high frequency (0.3 ms intervals).

2.5. Data Processing and Analysis

Data sets were sorted using Microsoft Excel and copied to worksheets of Origin™ version 2021 (OriginLab, Northampton, MA, USA), which was used for almost all subsequent elaborations. Data were preliminarily checked for outlier points, which were excluded from analysis using the "Mask data point" function of Origin™. Statistical assessment included the comparison of multiple samples using one-way or two-way (factors mutant and light regime) ANOVA, followed by post-hoc comparison of mean values using Tukey's test. The different variables were measured from 4 to 7 independent plants for each of the 16 combinations of wheat line and light regime. Two technical replicates were obtained for each plant and, to take into account that each plant was consequently represented twice for each analysed parameter, a conservative approach was chosen to assess the statistical significance of differences, fixing the statistical significance threshold at $P < 0.01$. The graphs presented in this report, either histograms or box charts, are based on the results of the descriptive statistics. Origin™ was also used for the data fitting analysis. The couples of variables were fitted with a linear function, but in specific cases other fitting models were checked (exponential, polynomial, rational functions). Effectiveness of fitting was checked using *Adj.* R^2 and the associated probability; each regression curve is reported with confidence bands at 95% probability. Pearson's *r* correlation matrixes were built using Microsoft Excel™; significant and very significant correlations were identified based on $P < 0.05$ and $P < 0.01$, respectively.

3. Results

An overview of OJIP traces is reported in Suppl. Fig. 1 and Suppl. Fig. 2 for the example of mature plants analysed at the 4th week. WT and mutant lines differed with respect to their absolute fluorescence emission (Table 1). The curve normalization on F_0 visualized the increment in F_V in all mutants (Suppl. Fig. 1-2).

3.1. PSII Antenna Size

The main expected physiological change in chlorophyll-deficient

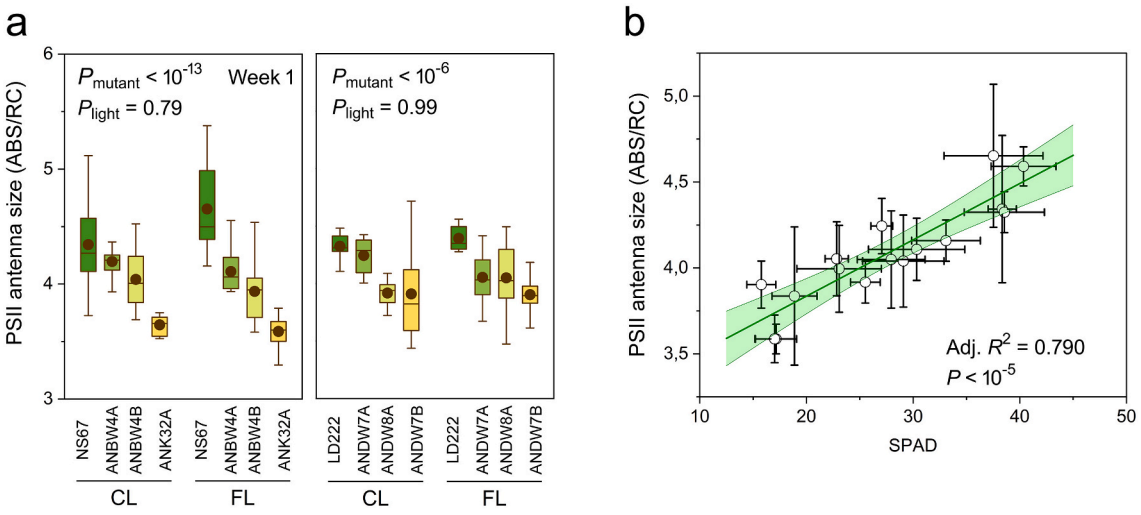

Fig. 2. PSII functional antenna size in young wild-type wheat (NS67, LD222) or their chlorophyll-deficient mutants grown under a continuous (CL) or fluctuating (FL) light regime. (a) PSII functional antenna size as light absorption per reaction centre (ABS/RC) at the first week of analysis. In the box charts, the box size is determined by the 25th and 75th percentiles, with whiskers at the 5th and 95th percentiles. The circle inside the box is the mean, the segment is the median (8–14 determinations). Results of statistical analyses were obtained with two-way ANOVA for the factors "mutant" and "light". (b) Correlation between ABS/RC and the chlorophyll content index SPAD at the first week of analysis; the green regression line is shown with 95% confidence bands. SPAD data were from Ferroni et al. [15]. (For interpretation of the references to colour in this figure legend, the reader is referred to the web version of this article.)

wheat is a reduction in the functional PSII antenna size, which was measured as the light absorption per reaction centre (ABS/RC). The time course of ABS/RC is reported in Suppl. Fig. 3. Wheat lines differed strongly from each other at the first week of analysis, when the PSII antenna size correlated with the leaf chlorophyll index (SPAD values from [15]; Fig. 2a-b). During the subsequent weeks, the PSII antenna size tended to decrease, especially in WT lines (Suppl. Fig. 4); this is an expected acclimative response to a higher light availability in plants growing closer to the light source. At the 4th week of analysis, ABS/RC was very similar in all plants, except ANK32A and, partly, ANDW7B (Fig. 3a). Because it is known that this collection of mutants tends to recover a WT-phenotype and the ABS/RC became indeed similar in all lines, we analysed the leaf chlorophyll in mature plants (Fig. 3b-c). The different severity of chlorophyll depletion in mutants was still visible and the chlorophyll *a/b* ratio was negatively correlated with the total chlorophyll content (Fig. 3d). The variability of the chlorophyll content parameters patently contrasted with the narrow range of ABS/RC variation: in the covariation graphs, all points aligned nearly horizontally within the ABS/RC range of [3.75–4.10], only except ANK32A (Fig. 3e-f).

Therefore, all mutants except ANK32A were able to recover a WT-like ABS/RC. Interestingly, normal ABS/RC could be achieved even in the presence of a lower chlorophyll content (e.g., ANDW7A).

3.2. Photochemical Activity and Photoinhibition of PSII

A higher F_V/F_M value was a very characteristic trait in all mutants as compared to WT wheat, stable over four weeks of analysis; therefore, data were pooled together for each wheat accession and light regime (Fig. 4a; Suppl. Fig. 5). The effect of the mutation was very evident, extremely significant and prevailed over that of the light regime. However, the latter also had a significant impact on F_V/F_M, in particular a tendency to a further small increase under FL, as visible in ANBW4B, ANDW7B and ANDW7A. We plotted the mean values of F_V/F_M against the values of SPAD (values from [15]; Fig. 4b). A very significant negative correlation linked F_V/F_M and SPAD index. F_V/F_M reflected closely the order of severity of the phenotype in both bread and durum wheat: the more severe the phenotype, the higher the F_V/F_M.

The F_V/F_M values were recorded also in the early afternoon, ca. 5 h after the first determination. During such time interval, the FL plants were exposed to ca. 80 lightflecks (Fig. 4c). Based on the current understanding of photosynthetic electron flow, the repetitive lightflecks may have caused as many events of PSII over-excitation and consequent reducing bursts [88]. Therefore, we compared the mutants with respect to the loss in F_V/F_M; this was <2% on average in all samples over 4 weeks without any significant effect due to the mutation or the light regime (Fig. 4d). The minimal PSII yield loss excluded differences in the susceptibility of PSII to photoinhibition or in other sustained NPQ forms.

3.3. Electron Transport Chain

To obtain information on the electron transport chain, the wheat lines were phenotyped using the relative fluorescence at the steps J and I after double normalization between O and P (Suppl. Fig. 1-2). Previous experimental evidence indicated that the reduction of the PQ pool starts at the J step, suggesting that the relative fluorescence V_J is determined by the availability of oxidised PQ molecules to reoxidise Q_A^- [20,85]. Consequently, ΔV_{JP} allows a comparison of the oxidised PQ pool size in wheat lines. Because the ΔV_{JP} values underwent developmental changes, and in particular, they were slightly increasing over time (Suppl. Fig. 6), the wheat lines were more easily compared at the 4th week (Fig. 5a). In bread wheat samples, uniform ΔV_{JP} values indicated nearly identical PQ pools in all plants; in fact, the double-normalized OJIP curves had an almost completely overlapping O-J phase (Suppl. Fig. 1). The same was true in durum wheat under FL but not under CL, with a smaller PQ pool in mutants than in LD222 (Fig. 5a, Suppl. Fig. 2).

ΔV_{IP} generally brings information on the reduction of the entire electron transport chain up to the acceptor side of PSI (ferredoxin and ferredoxin-NADP$^+$ oxido-reductase, FNR). Different from ΔV_{JP}, we found that, in wheat, ΔV_{IP} showed quasi-static values over the four weeks, generally higher in mutants than in WT lines (Suppl. Fig. 7). For homogeneity of data presentation, Fig. 5b shows ΔV_{IP} at the 4th week. Based on the most common interpretation of the thermal phase [71], this result was suggestive of more efficient electron transport from PSII to PSI end acceptors in mutants.

Interestingly, there was no obvious relation between the results obtained with ΔV_{JP} and ΔV_{IP} (Fig. 5a-b). Therefore, we compared the wheat lines with respect to the $\Delta V_{IP}/\Delta V_{JP}$ ratio. The physiological meaning of $\Delta V_{IP}/\Delta V_{JP}$ is unclear, but experimental evidence linked it to the activity of PSI that moves electrons from the reduced intersystem

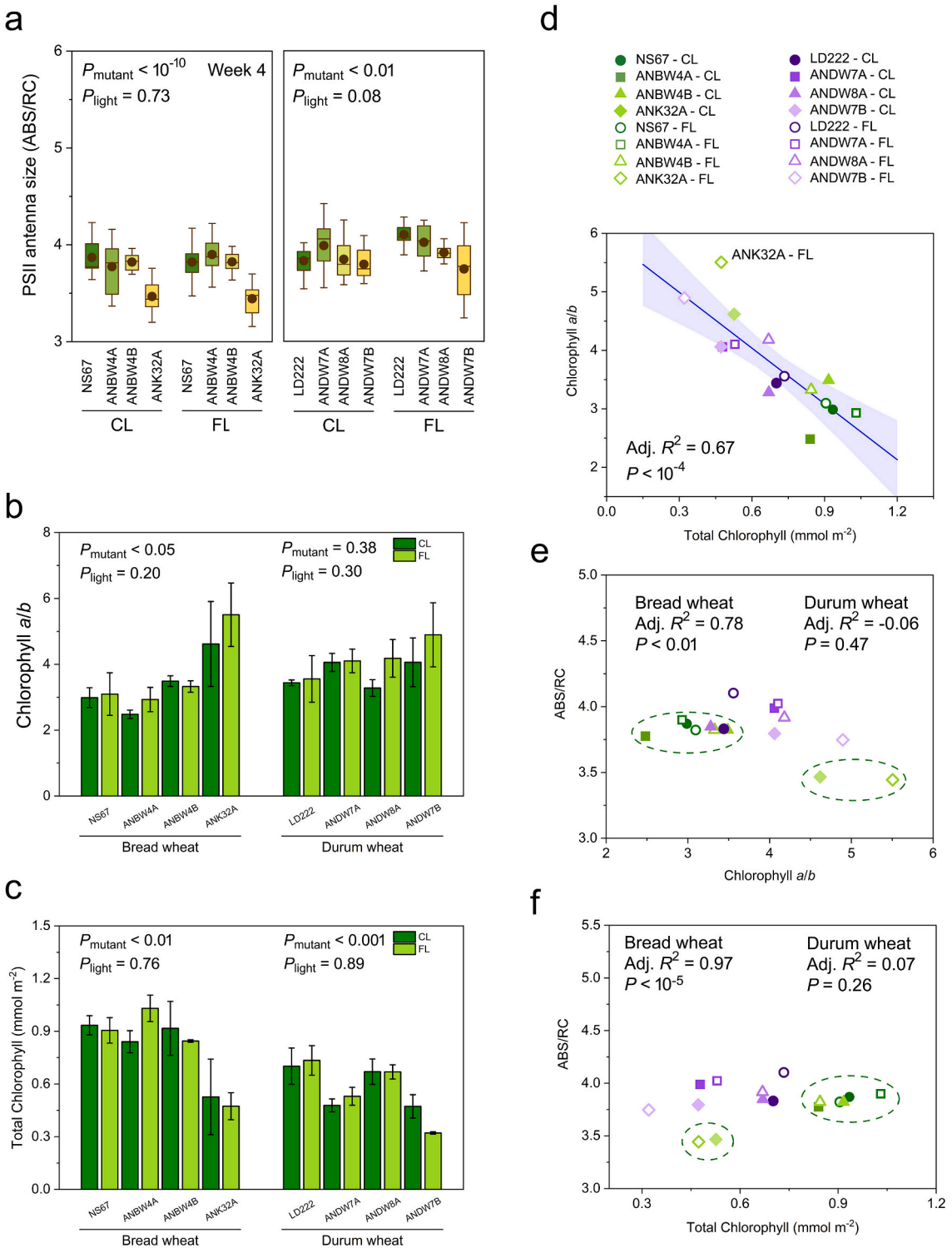

Fig. 3. Chlorophyll content and PSII functional antenna size in mature wild-type wheat (NS67, LD222) or their chlorophyll-deficient mutants grown under a continuous (CL) or fluctuating (FL) light regime. (a) PSII functional antenna size as light absorption per reaction centre (ABS/RC) at the fourth week of analysis. In the box charts, the box size is determined by the 25th and 75th percentiles, with whiskers at the 5th and 95th percentiles. The circle inside the box is the mean, the segment is the median (8–14 determinations). (b-c) Chlorophyll *a/b* molar ratio and total chlorophyll content (means ± SE of 2–4 determinations). (d) Covariation of chlorophyll *a/b* ratio and total chlorophyll content, with regression line and 95% confidence bands. The outlier point is indicated and corresponds to mutant ANK32A under FL. (e) Covariation of ABS/RC and chlorophyll *a/b* ratio; two bread wheat point clouds are circled with a dashed line. (f) Covariation of ABS/RC and total chlorophyll content; two bread wheat point clouds are circled with a dashed line. Results of statistical analyses in a-c were obtained with two-way ANOVA for the factors "mutant" and "light". Results of linear regression are shown in d-f.

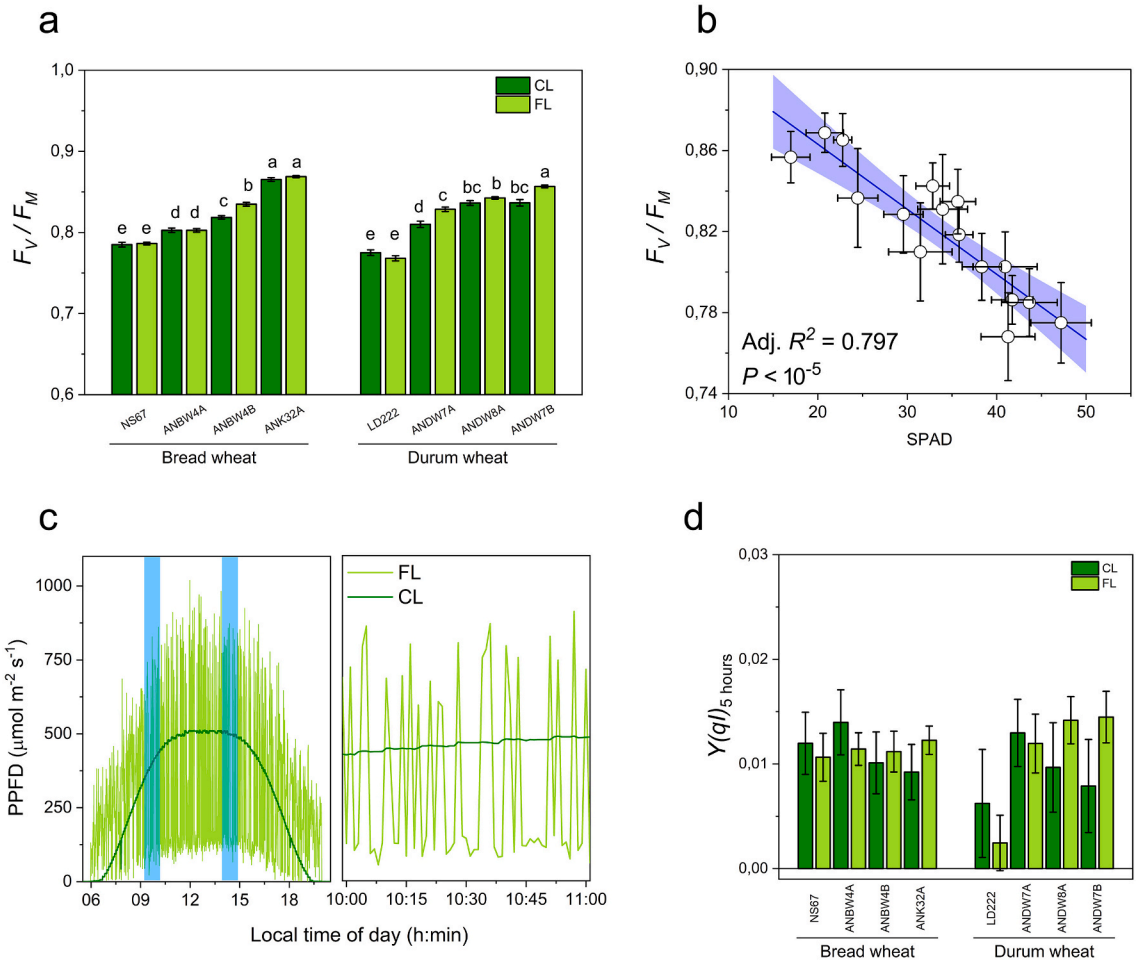

Fig. 4. PSII photochemistry in wild-type wheat (NS67, LD222) or their chlorophyll-deficient mutants grown under a continuous (CL) or fluctuating (FL) light regime. (a) Maximum quantum yield of PSII (F_V/F_M). (b) Correlation analysis of F_V/F_M with the SPAD index of leaf chlorophyll content (data from [15]). (c) Example of a daily variation in light intensity in the two sectors of the growth chamber: in the left panel, the light blue bands indicate the two times of fast fluorescence induction analysis; in the right panel, a detail of the irradiance variation pattern is shown during one hour. (d) Loss of PSII quantum yield during 5 hours of growth under CL or FL, $Y(qI)_{5\ hours}$. In a and d, values are means ± SE of 32–56 determinations. In a, different letters indicate statistically significant differences based on Tukey's post-hoc test run separately for bread and durum wheat lines; in d, no significant differences occurred with respect to $Y(qI)_{5\ hours}$. (For interpretation of the references to colour in this figure legend, the reader is referred to the web version of this article.)

electron acceptors (PQ, Cytochrome b_6f, plastocyanin) to the final electron acceptors of PSI (mainly ferredoxin and FNR; e.g., [20]. In wheat, $\Delta V_{IP}/\Delta V_{JP}$ was a quite dynamic parameter over the four weeks of monitoring, but the relative changes between mutants were mostly confirmed week after week (Fig. 5c-d). An interesting exception occurred in the bread wheat lines under FL, with a progressive divergence of ANBW4B from NS67. As shown in Fig. 5e, reporting data from the 4th week, $\Delta V_{IP}/\Delta V_{JP}$ was very sensitive to the effect of the mutation and light regime: progressively higher values closely matched the known severity order of the mutant lines.

Given the higher ΔV_{IP} in mutants, we analysed if the overall pool of intersystem electron transporters had also increased. The F_V-normalized area *Sm* is considered as a proxy of the number of electron transporters per electron transport chain [70]; for a discussion on *Sm* see also [27]. The inference of higher *Sm* was correct in bread wheat lines, particularly in ANBW4B under FL and in ANK32A, but *not* in durum wheat. In all durum wheat samples, ANDW7B included, the electron transporters pool had the same size (Fig. 5f). The covariation of parameters $\Delta V_{IP}/\Delta V_{JP}$, ΔV_{JP}, and *Sm* is reported in Fig. 6. In bread wheat, the higher $\Delta V_{IP}/\Delta V_{JP}$ was supported by an increased availability of electron transporters; very differently, in durum wheat the higher $\Delta V_{IP}/\Delta V_{JP}$ did not depend on more electron transporters, but rather on a smaller PQ pool size, ΔV_{JP}, associated to bigger ΔV_{IP}.

The comparison of the first and second F_V/F_M obtained with the double hit method can provide some rough information about the ability of wheat plants to re-oxidise the PQ pool. We assume that at the end of the first pulse all Q_A has been reduced (although OJIP traces showed some quenching, see Suppl. Fig. 1-2). The fraction of lost F_V/F_M (B_O) was not constant over the four weeks but decreasing, which could indicate an improved control of the PQ pool redox state during the plant development (Suppl. Fig. 8). However, ANK32A and ANDW7B evidently tended to maintain higher values than the corresponding WT lines. In Fig. 7a-b, the first (F_V/F_M) and second pulse (F_V*/F_M*) are compared at the 4th week. Interestingly, F_V*/F_M* was nearly the same in all wheat lines, without any significant effect due to the mutation or light regime. Conversely, the F_V/F_M - F_V*/F_M* difference closely matched the severity of the mutants. In general, the light regime did not influence much this value, with the noticeable exception of ANDW7B, in which the FL regime induced a further increment (Fig. 7a-b).

$\Delta(B_O)$ compares B_O between the morning and the afternoon. In general, $\Delta(B_O)$ was small and quite erratic in the wheat lines (Fig. 7d). However, in most cases the tendency was towards negative $\Delta(B_O)$, suggesting a small gain in PQ redox control during the day.

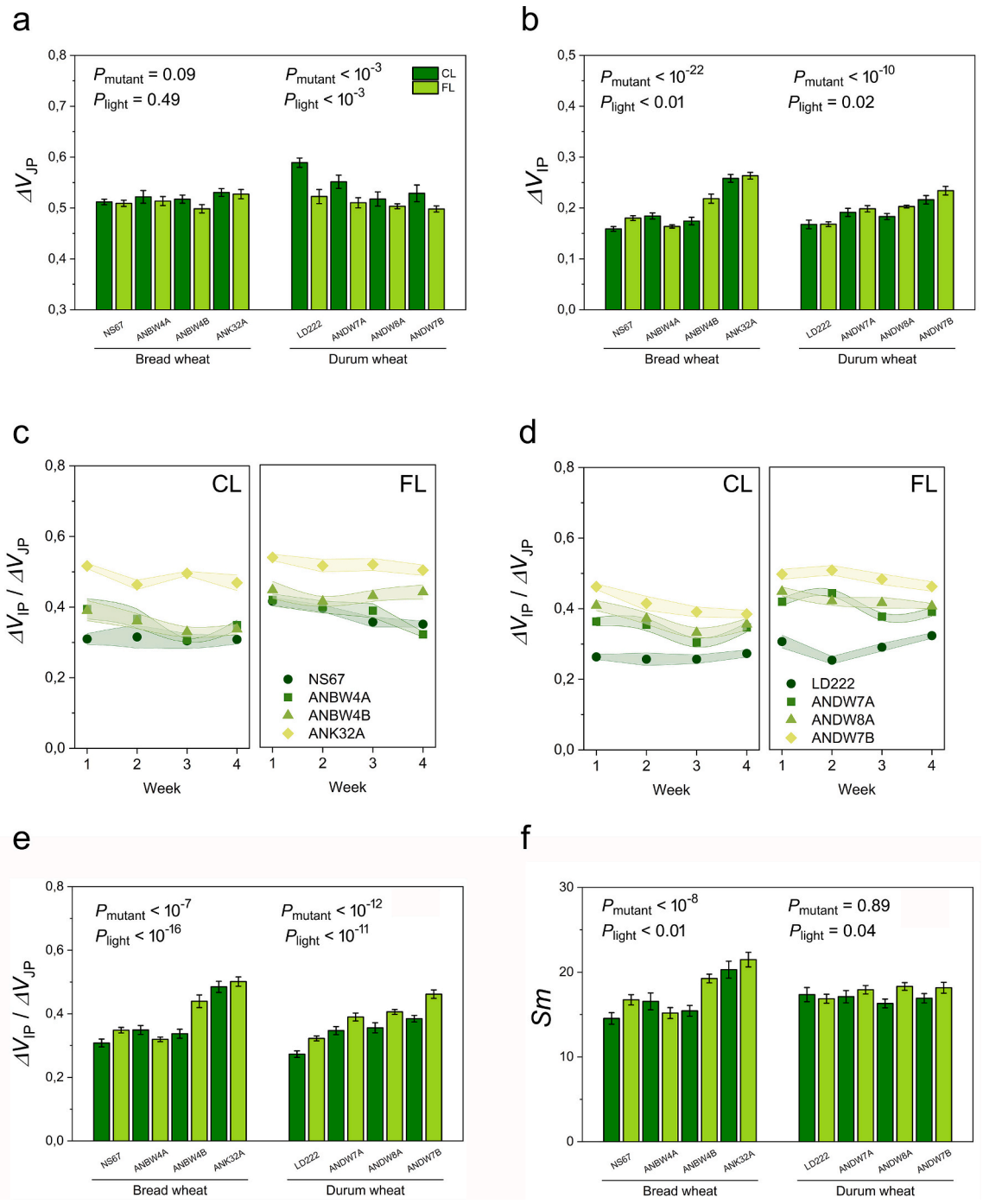

Fig. 5. Electron transport analysis based on OJIP transients recorded from wild-type wheat (NS67, LD222) or their chlorophyll-deficient mutants grown under a continuous (CL) or fluctuating (FL) light regime. (a) Complement to one of the relative fluorescence at step J ($\Delta V_{JP} = 1 - V_J$) and (b) at step I ($\Delta V_{IP} = 1 - V_I$) at the fourth week of analysis. (c-d) Time course of the ΔV_{IP} /ΔV_{JP} ratio during four weeks of monitoring in bread (c) and durum wheat lines (d). Values are means; bands represent joined SE of the means. (e) ΔV_{IP} /ΔV_{JP} ratio at the fourth week of analysis. (f) Normalized area *Sm* at the fourth week of analysis. In all histograms, values are means ± SE of 8–14 determinations. Results of statistical analyses were obtained with two-way ANOVA for the factors "mutant" and "light".

3.4. Correlative Analysis

The interpretation of the parameters obtained from the OJIP transients can benefit from the context provided by other analyses performed using complementary methods during the same experiment. The correlative analysis can be particularly useful to explore possible mechanistic relations involving $\Delta V_{IP}/\Delta V_{JP}$, which emerged as a very straightforward index to characterize the mutants. Among the different parameters we have previously reported [15], the following were used to build Pearson's *r* correlation matrixes:

- the final aboveground biomass,
- the SPAD index of leaf chlorophyll content,
- the variation in PQ reduction [$\Delta Y(NO)$] upon a rapid light rise from 539 to 1960 µmol photons m^{-2} s^{-1} (rapid light curve based on Dual-PAM analysis of modulated chlorophyll fluorescence),

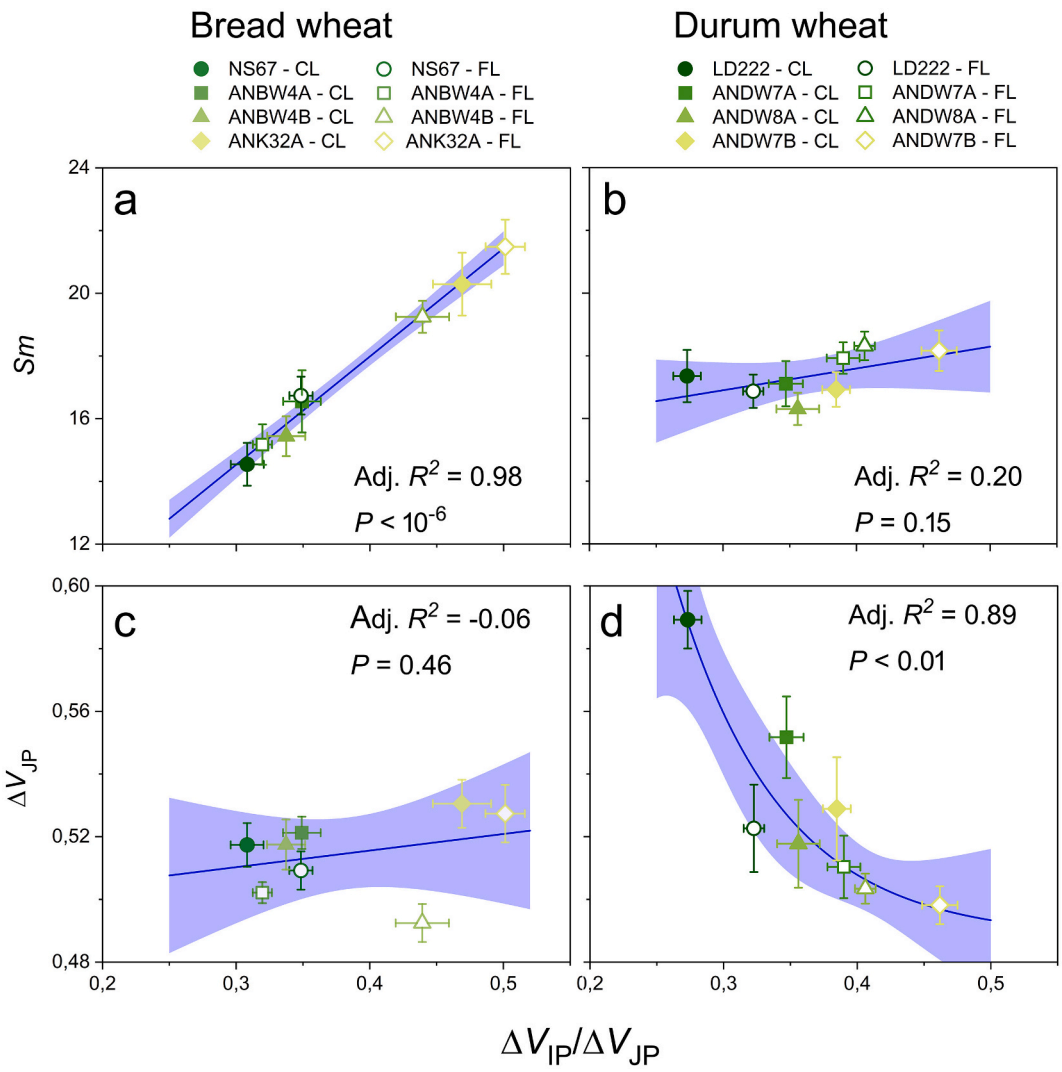

Fig. 6. Intersystem electron transport in wild-type wheat (NS67, LD222) or their chlorophyll-deficient mutants grown under a continuous (CL) or fluctuating (FL) light regime. (a-b) Covariation of *Sm*, a proxy of the number of electron carriers per electron transport chain, and $\Delta V_{IP}/\Delta V_{JP}$ in bread (a) and durum wheat (b). (c-d) Covariation of $\Delta V_{IP}/\Delta V_{JP}$ and ΔV_{JP} in bread (c) and durum wheat (d). In all cases, data were obtained from the fourth week of monitoring and the values are means with SE. The result of the linear regression in (a-c) and of the exponential decay fitting in (d) is shown with 95% confidence bands.

- the variation in acceptor-side-limited PSI quantum yield [$\Delta Y(NA)$] upon a rapid light rise from 539 to 1960 μmol photons m^{-2} s^{-1} (rapid light curve based on Dual-PAM analysis of P700 absorbance),
- the steady-state fraction of electron transport deviated to alternative sinks (J_A/J_{PSII}) (simultaneous analysis of gas exchange and chlorophyll fluorescence based on Licor 6400 analysis),
- the relative leaf content of photo-oxidizable PSI (maximum P700 signal – *Pm* – based on Dual-PAM analysis in the dark-acclimated state; *Pm* was normalized on the SPAD index),
- the steady-state quantum yield ratio of PSI and PSII, *Y(PSI)/Y(PSII)* (simultaneous chlorophyll fluorescence and P700 analysis based on Dual-PAM).

Because the comparative OJIP analyses already showed the specificity of bread and durum wheat lines (Fig. 6), the parameters obtained with the two species were analysed separately in Fig. 8. The values used are from the 4th week of analysis.

Particularly interesting and shared by both wheat species was the very strong negative correlation between $\Delta V_{IP}/\Delta V_{JP}$ and the plant biomass. In bread wheat, it was even stronger than the relation between the biomass and the chlorophyll content or F_V/F_M. The $\Delta V_{IP}/\Delta V_{JP}$-biomass plots confirmed the significant and strong linear relation between the two variables in durum wheat lines. The relation was likewise strong in bread wheat, but the plot was best fitted with a rational function (Fig. 9).

An important aspect to investigate was the possible negative relation between $\Delta V_{IP}/\Delta V_{JP}$ and ABS/RC (see [61]). The correlation analysis could be in favour of it in bread wheat but was in disfavour in durum wheat (Fig. 8). The point density plot in Fig. 10a shows that this result was caused by ANK32A, which fell outside the main point cloud. Inside the latter, the statistical analysis could not support any significant relationship between ΔV_{IP} and ABS/RC. The same conclusion is valid for the derived ratio $\Delta V_{IP}/\Delta V_{JP}$.

A special attention was paid to $\Delta Y(NO)$, which already provided evidence for the defective electron transport control in the same mutants [15,98]. In both wheat species, a strong relationship linked $\Delta Y(NO)$ with the lost PSII yield following the second pulse in the double hit protocol, directly supporting the latter as a parameter proportional to the ability to re-oxidise the PQ pool (Fig. 8). Very interestingly, $\Delta V_{IP}/\Delta V_{JP}$ was linearly correlated with both parameters (Fig. 10b-c).

No significant correlation with OJIP-derived electron transport parameters was found for $\Delta Y(NA)$ (Fig. 8). In durum wheat, a significant relationship linked the alternative electron transport J_A/J_{PSII} with ΔV_{IP}, $\Delta V_{IP}/\Delta V_{JP}$ and *Sm* (Fig. 8).

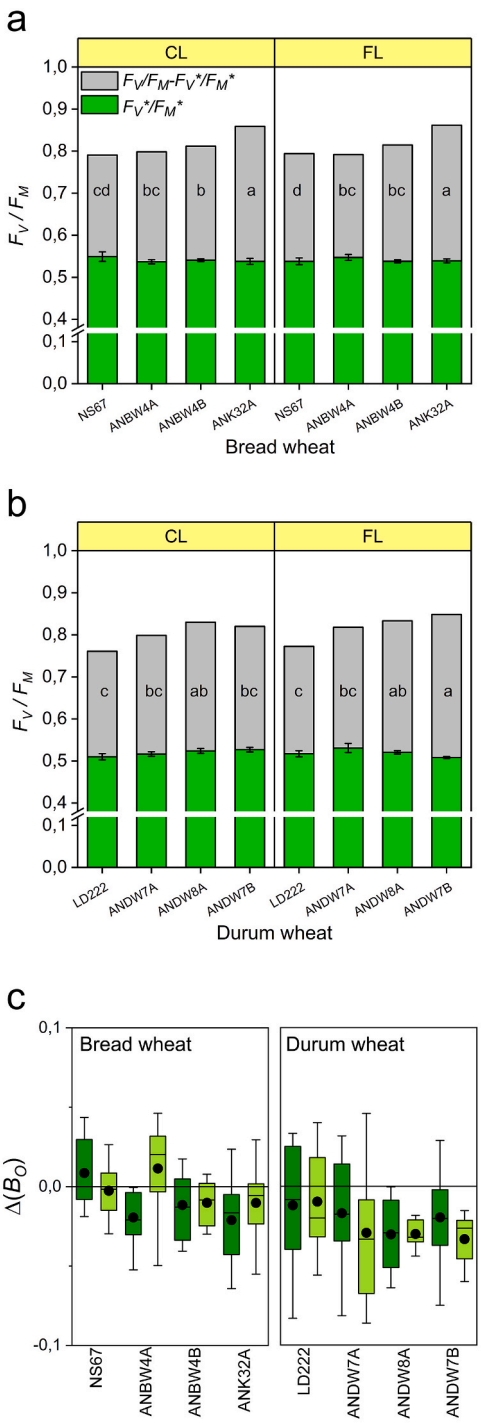

Fig. 7. Results of the double-hit method probing of PSII photochemistry in wild-type wheat (NS67, LD222) or their chlorophyll-deficient mutants grown under a continuous (CL) or fluctuating (FL) light regime. (a-b) PSII quantum yield recorded after the second pulse (F_V*/F_M*) and the difference with the first pulse (F_V/F_M*-F_V*/F_M*) in plants at the 4th week of experiment. Different letters indicate statistically significant differences with respect to F_V/F_M-F_V*/F_M* based on Tukey's post-hoc test; no significant differences occurred with respect to F_V*/F_M* in both bread and durum wheat lines. Values are means (N = 8–14); error bars are SE. (c) Afternoon-to-morning variation in the lost fraction of PSII photochemistry (B_O) upon a second pulse (5 h between the two determinations).In the charts, the box size is determined by the 25th and 75th percentiles, with whiskers at the 5th and 95th percentiles. The circle inside the box is the mean, the segment is the median.

The correlation analysis pointed to the absence of any significant relation between the relative amount of photo-oxidizable PSI and ΔV_{IP} or $\Delta V_{IP}/\Delta V_{JP}$ (Fig. 8). Interesting was the result of the correlations involving the *Y(PSI)/Y(PSII)* ratio, which is a functional hallmark for the defective CEF [96,98]. $\Delta V_{IP}/\Delta V_{JP}$ correlated negatively with *Y(PSI)/Y(PSII)*.

3.5. Analysis of Simultaneous Fast Fluorescence Transients and P700$^+$ Kinetics

Increased ΔV_{IP} and, even more, $\Delta V_{IP}/\Delta V_{JP}$ emerged as key features of the wheat mutant collection and were also sensitive to the light regime. To help interpret the changes in $\Delta V_{IP}/\Delta V_{JP}$ we analysed the P700$^+$ accumulation kinetics during the induction of the OJIP transient. The detailed kinetics analysis was focused on the wheat lines with extreme phenotypes, ANDW7B and ANK32A, which are approximately equivalent in terms of biomass yield under CL (ca. 55%). Conversely, the phenotype severity of ANDW7B is exacerbated by a FL regime, while that of ANK32A is not (Table 1; [15]). Despite the different probing method – modulated fluorescence –, the OJIP traces were similar to those obtained with a continuous excitation fluorometer, in particular the wider I-P phase in the mutants was evident (Fig. 11a-c).

In Fig. 11a and d, the traces obtained from the WT line LD222 are compared between CL and FL. From the onset of the saturation pulse, the P700$^+$ concentration rose rapidly up to a transitory steady state. The P700$^+$ accumulation indicated a limitation to the re-reduction due to the lack of reduced electron transporters, and, accordingly, it corresponded to the O-J phase and part of the J-I phase, when the PQ pool is expected to be still largely oxidised. At the P700$^+$ plateau, the rates of P700 oxidation and re-reduction are equal, meaning that electrons are being made available from the PQ pool. The subsequent I-P phase is dominated by the reduction of P700$^+$, which is completed at the P step. Growth under FL had two major consequences on the P700$^+$ accumulation kinetics: (a) the initial P700 oxidation became slower (Fig. 11a); (b) the plateau was reached later and was longer (Fig. 11d). Likewise, the rate of fluorescence increase during the I-P rise, related to the reduction of PSI end acceptors, became evidently slower under FL than CL (Fig. 11j).

Under CL, in ANDW7B the plateau of P700$^+$ accumulation was very short, and the subsequent P700 re-reduction was completed approximately 50 ms earlier than in LD222 (Fig. 11b, e). The higher reduction rate of PSI acceptors was confirmed by the faster kinetics of the I-P rise (Fig. 11k). However, the end acceptors pool was much larger than in LD222 (Fig. 11n). Interestingly, growth of ANDW7B under FL resulted in minor changes, i.e., slightly slower P700 re-reduction and minimally slower I-P phase.

Negligible difference in P700 kinetics between CL and FL also characterized ANK32A, again showing a very fast re-reduction of P700 (Fig. 11c, f). However, different from ANDW7B, under FL a slowing down of the I-P rise occurred after 50 ms (visible also in the P700$^+$ kinetics).

In all analysed lines, no relevant difference was found for the J-I kinetics (Fig. 11g-i). The PSI acceptor pool size, estimated from the I-P amplitude after O-I normalization [84], was larger in the mutants than in the WT line (Fig. 11m-o).

4. Discussion

4.1. Mature Chlorophyll-Deficient Wheat Mutants Are Hardly Distinguished Based on ABS/RC

The scientific literature is rich in reports on *chlorina* mutants of several species, including major Poaceae crops, such as wheat, rice and barley. In some cases, mutants specifically lack chlorophyll *b*; in others there is a decrease in the general chlorophyll content, which is secondarily accompanied by higher chlorophyll *a*/*b* ratio. Chlorophyll *b* is synthesized with leftover chlorophyll *a* after the assembly of the PSI

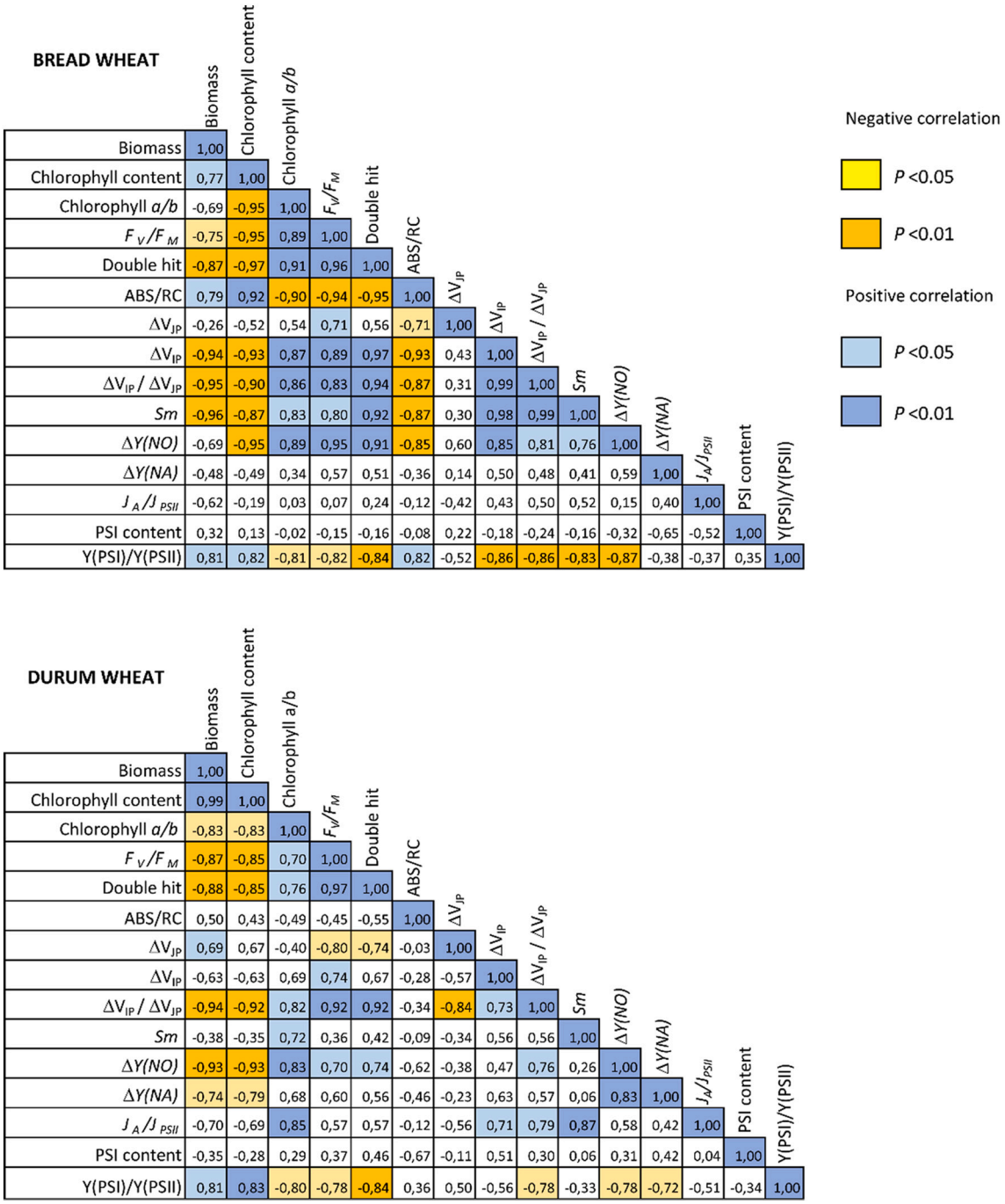

Fig. 8. Matrix of Pearson's *r* correlation coefficients of photosynthetic parameters in bread and durum wheat lines. For the definition of the variables, see 3.4. "Double hit" refers to the PSII quantum yield lost in dark-acclimated samples upon application of a second saturating pulse 500 ms after the first pulse. Correlations were analysed using mean values at the 4th week of analysis.

and PSII cores, thus allowing the subsequent assembly of the chlorophyll *a/b*-binding LHCs, principally LHCII [14]. Consequently, a negative relationship links chlorophyll *a/b* ratio and total chlorophyll content (Fig. 3d). In chlorophyll-deficient mutants, the higher chlorophyll *a/b* ratio associated with reduced chlorophyll content is generally treated synonymous with a reduced antenna of PSII [2,14,19,37,78,79]. This link is confirmed in transgenic *Arabidopsis thaliana* with reduced amount of LHCII subunits Lhcb1/2, chlorophyll *a/b* ratio increased from 3.2 to 4.0, chlorophyll content decreased by 20%, and halved functional PSII antenna size [4]. However, our analysis indicates that the mature wheat lines cannot be distinguished based on their ABS/RC, except ANK32A (Fig. 3e, f). In WT lines, ABS/RC reveals the acclimative decrease in PSII antenna size in new leaves of taller plants exposed to a higher light intensity (Suppl. Fig. 3). In mutants, such effect is less evident probably because of the gradual compensation of the genetic lesion in subgenome A or B by the functional homoeologous genes in the other subgenome(s), leading to increasing chlorophyll content [15,98]. Mutants such as ANDW7A, with 30% less chlorophyll but normal ABS/RC, may suggest an intrinsic capacity of wheat to adjust the PSII antenna system in case of moderate chlorophyll deficiency. Moreover, changes in antenna homogeneity, connectivity, interaction with both photosystems could influence ABS/RC [70,95]. While these aspects deserve further investigation, it is clear that ABS/RC was a weak phenotypic index in our conditions, and parameters, such as F_V/F_M and $\Delta V_{IP}/\Delta V_{JP}$, could not be merely

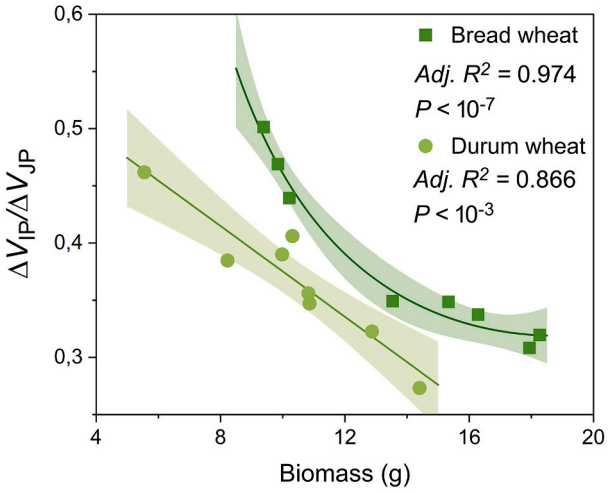

Fig. 9. Covariation of $\Delta V_{IP}/\ \Delta V_{JP}$ with the final aboveground plant biomass The $\Delta V_{IP}/\Delta V_{JP}$ values used for the analysis are the means recorded at the 4th week of monitoring. Biomass values are those reported in Ferroni et al. [15] and obtained from the same experiment. The fitting function was linear for durum wheat, rational for bread wheat.

explained based on differences in effective PSII antenna size.

4.2. *In Chlorophyll-Deficient Wheat, Higher F_V/F_M cannot Reliably Indicate a Superior PSII Activity*

The literature is not consistent with respect to F_V/F_M in chlorophyll- or antenna-deficient mutants, including the case of higher values than the WT, interpreted as higher PSII photochemical activity (e.g., [93,94]). In our study, it is quite improbable that the higher F_V/F_M reveals a genuinely superior PSII photochemistry in mutants, which would contrast with their lower carbon fixation capacity and biomass accumulation [15,98]. In general, in chlorophyll-deficient mutants, F_V can be affected by factors that make it difficult to exactly equate F_V/F_M to the quantum efficiency of PSII. The primary cause of a higher F_V/F_M is the low PSI/PSII ratio [52] characterizing chlorophyll- and antenna-deficient plants, already demonstrated also in ANK32A [6,19,48,78,79,97]. Moreover, the very neat separation between grana stacks and long arrays of single thylakoids in ANK32A and ANDW8A [15] is strongly suggestive of a hindered energy spillover from PSII to PSI, again resulting in higher F_V/F_M [12,28]. In mutants, the lower PSI/PSII ratio is generally interpreted as a compensatory mechanism against the decreased light-harvesting capacity of PSII, which causes an excessive excitation of PSI [2,6,48,78,79]. However, we show that F_V/F_M remains high also when the functional PSII antenna size and the chlorophyll content have been restored to WT values (e.g., ANDW8A,

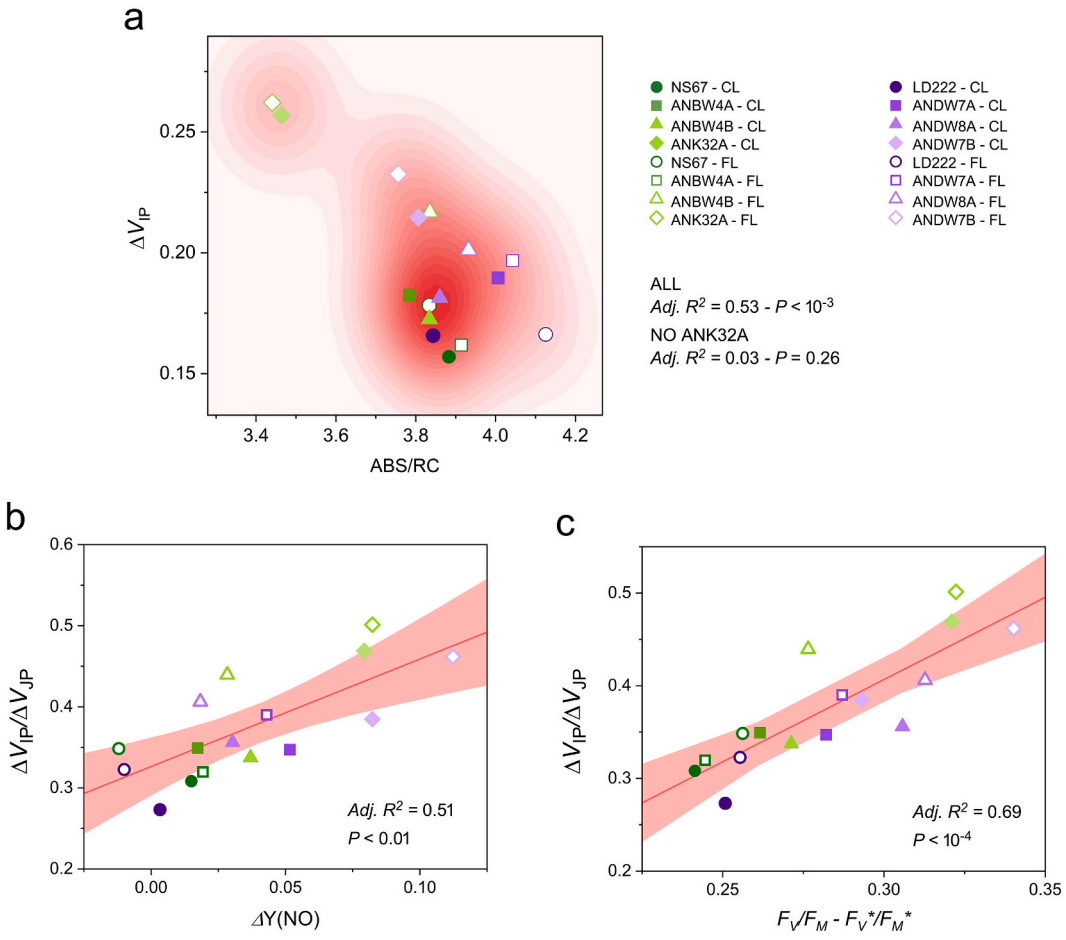

Fig. 10. Correlative analyses focused on the I-P phase of the fluorescence transient in mature wheat lines (4th week of monitoring). (a) Covariation of ΔV_{IP} with the effective PSII antenna size (ABS/RC). The data plot was analysed with a kernel density estimation, that shows a pattern neatly separating ANK32A from all other wheat lines. The results of the correlation analysis with or without ANK32A are reported. (b) Covariation of $\Delta V_{IP}/\ \Delta V_{JP}$ with the yield $\Delta Y(NO)$ of non-regulatory energy dissipation in PSII upon a rapid rise in irradiance (539 to 1960 μmol photons m^{-2} s^{-1}), related to plastoquinone reduction state. $\Delta Y(NO)$ are values reported in Ferroni et al. [15] and obtained from the same experiment. (c) Covariation of $\Delta V_{IP}/\Delta V_{JP}$ with the PSII quantum yield lost following application of a second pulse in the double hit protocol (F_V/F_M - F_V*/F_M*, see main text for details). In b and c, the regression line is shown with 95% confidence bands.

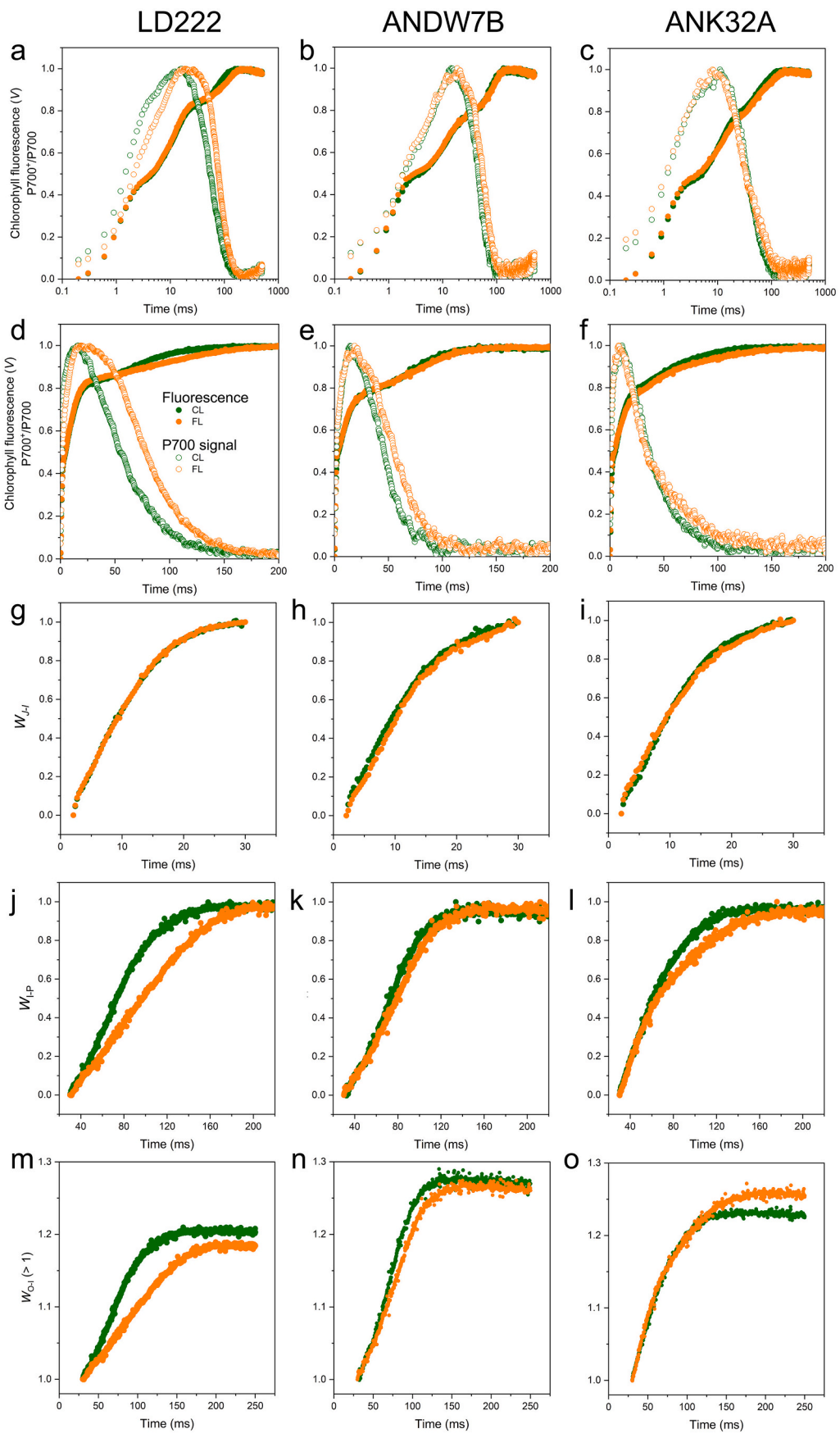

Fig. 11. Comparative analysis of simultaneous traces of P700 redox state and fast chlorophyll *a* fluorescence in WT (LD222) and chlorophyll deficient (ANDW7B and ANK32A) mature durum wheat lines cultivated under a continuous (CL) or fluctuating (FL) light regime. (a-c) Fast chlorophyll fluorescence V normalized by F_0 and F_M (OJIP transient) and $P700^+$ accumulation kinetics shown on a logarithmic time scale. (d-f) The same traces as in a-c shown on a linear time scale. (g-i) Fluorescence rise kinetics normalized by F_J (2 ms) and F_I (30 ms) as $W_{J\text{-}I}$. (j-l) Fluorescence rise kinetics normalized by F_I (30 ms) and F_M as $W_{I\text{-}P}$. (m-o) Fluorescence rise kinetics normalized by F_0 and F_I (30 ms) as $W_{O\text{-}I}$ shown in the I-P phase range, i.e., at $W_{O\text{-}I} > 1$.

Fig. 4a). This observation suggests more profound impacts of an altered chlorophyll biosynthesis than the mere downsizing of the PSII antenna.

4.3. I-P Phase and Acclimative Response of the electron Transport to a FL Regime

In the mainstream Q_A model, the I-P phase is attributed to the reduction of the end acceptors of PSI [34,71,84]. Alternative models exist [61,62,64,68,86], but the importance of the relative PSI activity in determining the I-P phase amplitude is well supported experimentally and, per extension, frequently associated to the PSI/PSII ratio [9,43,50,54,59,60]. $\Delta V_{IP}/\Delta V_{JP}$ has likewise been used as an indicator of the relative PSI activity [20]. With $\Delta V_{IP}/\Delta V_{JP}$, the PSI-related I-P phase is somehow normalized on the pool of oxidised PQ, as estimated from ΔV_{JP} [85]. In our experiment with wheat, two factors are responsible for increased $\Delta V_{IP}/\Delta V_{JP}$: the genetic lesion affecting chlorophyll biosynthesis and the acclimation to FL.

Growth under FL exposes plants to a continuous and unpredictable series of light- and shadeflecks. To prevent possible PSI damage due to electron bursts, the acclimative adjustments to FL should: (a) alleviate the PSI acceptor-side limitation, enhancing the downstream electron sinks, and (b) enhance the PSI donor-side limitation, decreasing the number of electrons that reach PSI mainly through the downregulation of cytochrome b_6f [17,65,87]. A central role is acknowledged to the CEF around PSI, which is also a strong inducer of PSII downregulation through the ΔpH-dependent generation of NPQ [44,87]. Fast chlorophyll *a* fluorescence probes the photosynthetic membrane in the dark-acclimated state, in which electrons cannot flow beyond FNR [60], offering a view of properties intrinsic to the structure of the electron transport chain from PSII to FNR. The $\Delta V_{IP}/\Delta V_{JP}$ increase under FL in WT lines, though relatively small, is evidence that the electron transport chain has undergone acclimative changes (Fig. 5e). Under FL, the slower reduction rates of $P700^+$ and PSI terminal acceptors (I-P phase) indicate that, already in the dark-acclimated state, the electron transport is limited compared with CL samples (Fig. 11d, j). Possible explanations can be a lower input of electrons into the chain from PSII related to higher PSI/PSII ratio, and/or a narrower "bottleneck effect" at the cytochrome b_6f. Very interestingly, the membrane seems already predisposed to the PSI donor-side limitation, which CEF and ΔpH will further promote upon exposure to lightflecks. Together with modulations of the mobile carriers (PQ pool in durum wheat or all pools in bread wheat, Fig. 5a, f), this may influence the kinetics properties related to the electron flow control, which is worth to be further studied.

4.4. The Enlargement of the PSI End Acceptor Pool Occurs in Chlorophyll-Deficient Mutants to Relieve their Altered electron Flow

In chlorophyll-deficient wheat, higher $\Delta V_{IP}/\Delta V_{JP}$ and ΔV_{IP} occur in the unusual frame of a lower relative content and activity of PSI, therefore challenging the most common use of ΔV_{IP} as a semi-quantitative indicator of the relative PSI amount/activity [9]. A causal relationship between smaller PSII antennae and higher ΔV_{IP} (see e.g., OJIP traces in [3], is ruled out by the contrasting developmental changes in ABS/RC and ΔV_{IP}, along with the lack of correlation between the two parameters (Suppl. Figs. 3,7; Fig. 10a). The interpretation of ΔV_{IP} and the derived $\Delta V_{IP}/\Delta V_{JP}$ is helped by the simultaneous kinetics of OJIP transient and P700 redox state. In mutants, the fast transition to the prevailing P700 re-reduction proves that the electrons are conveyed very promptly from PQH_2 to $P700^+$ and, similarly, the faster I-P rise indicates that the electrons flow easily up to the end acceptors, mainly ferredoxin and FNR [58,59,95,96]; Fig. 11d-f, j-l). This kinetics is strongly suggestive of an enlarged bottleneck at the cytochrome b_6f, probably also related to a high amount of PSII feeding the chain. It can be surprising that the low relative amount of PSI does not constrain the fast electron flow to the end acceptors. PSI photoinactivation experiments led to the same conclusion, revealing that a halved amount of photochemically active PSI had negligible impact on the OJIP transient, with no change in the I-P phase [97]. Shimakawa and Miyake [66] demonstrated that the PSI amount is in excess of the need for photosynthesis in intact leaves, while the surplus ensures the accumulation of oxidised PSI, which acts as a safe thermal dissipator. Therefore, while anomalously low PSI/PSII ratio negatively affects photoprotection [6,66], it can be still permissive to an effective electron flow from plastocyanin to end acceptors. The consequence is that the I-P phase certainly relates to the PSI activity that moves electrons from plastocyanin to ferredoxin and FNR, but ΔV_{IP} does not always provide reliable information about the relative PSI content or PSI/PSII stoichiometry. Differently, the amplitude of the I-P phase can be informative on the relative pool of PSI end electron acceptors [83,95–97]. In WT plants, end acceptor pool and PSI content are modulated consistently with each other and with the carbon fixation capacity, for example during sun-shade acclimation, thus explaining the correlation between ΔV_{IP} or $\Delta V_{IP}/\Delta V_{JP}$ with PSI/PSII ratio [8,54,95,96]. The chlorophyll biosynthesis disturbance in wheat mutants illustrates that the connection between relative amount of PSI and pool size of end acceptors can be lost.

The main defect of the electron transport in chlorophyll-deficient wheat lines is the excessive linear electron flow, promoting a tendency to chronic states of PSI over-reduction [6,15,98]. Very interestingly, the ineffective control of the linear electron transport is not only related to a limited capacity to induce CEF but is also found in the dark-acclimated state (faster electron flow, correlation between $\Delta Y(NO)$ and the lost F_V/F_M; Figs. 8, 11), and therefore intrinsic to the thylakoid membrane organization. The molecular causes are unknown and could include alterations in relative amount of cytochrome b_6f, or modified supramolecular interactions of complexes affecting the cytochrome b_6f activity (e.g., with PSI or CEF effectors), or changes in its distribution between thylakoid domains (e.g., linked to anomalous thylakoid assembly) (for review on cytochrome b_6f, [41]). Without any parallel increase in carbon assimilation [15], the enlargement of the end acceptor pool could seem a futile investment of metabolic energy. Nevertheless, the linear correlation between $\Delta V_{IP}/\Delta V_{JP}$ and the degree of disturbance of the PQ redox state (Fig. 10b-c) suggests that a more capacitive pool of end electron acceptors may have a compensatory role of the electron transport defect. Given the lower ability of mutants to exploit the donor-side limitation of PSI, a feedback response to the PSI over-reduction can be the alleviation of the acceptor-side PSI limitation. Some mutants have an increased ability to drive electrons to sinks alternative to photosynthesis and photorespiration (J_A/J_{PSII}, [15]), but not, e.g., ANK32A, despite the highest ΔV_{IP} and $\Delta V_{IP}/\Delta V_{JP}$. We suggest that the accumulation of the PSI end acceptors might be protective *per se*. Especially the abundance of FNR can be regarded as a critical component to prevent the PSI photoinactivation and promote light stress tolerance [33,39,51,56]. Emerging evidence suggests that the photoprotective role of FNR is not limited to the forward electron flow to the NADPH-consuming metabolisms. The over-expression of FNR in tobacco plants caused only a moderate increase in $NADP^+$ reduction and no effect on CO_2 assimilation but resulted in enhanced tolerance to photodamage [56]. Therefore, it was proposed that increased levels of FNR can directly provide a sink pool to maintain P700 in the safe oxidised state, while also helping remove radical species [56,57]. This hypothesis well matches our observations in wheat mutants, revealing the accumulation of PSI end acceptors, perhaps principally FNR, as a novel compensatory mechanism against the deregulated electron flow in chlorophyll biosynthesis mutants. The OJIP analysis clearly offers an electron transport snapshot in a condition in which electrons cannot flow beyond FNR [59], and therefore the functional relevance of the ferredoxin and FNR accumulation in mutants is not directly evident. However, some indirect information supporting the beneficial increase of end acceptors can be obtained comparing ANBW4B and ANDW7B, which share the same mutation at locus *cn-B1b*. The influence of the additional genome D characterizing the hexaploid bread wheat on photosynthetic performance and, particularly, its response to stress is not easily predictable

[5,10,15,42,89]. In bread wheat mutants, the increase in PSI end acceptors is part of a general enlargement of the electron carriers pool per chain, *Sm*; in durum wheat, the overall carrier abundance does not change, but the PQ pool size, ΔV_{JP}, is downregulated (Fig. 6). Under FL, the changes in OJIP transients due to the mutation combine with those due to the FL regime, both promoting higher $\Delta V_{IP}/\Delta V_{JP}$. This further enlargement of the end acceptors pool has very likely a metabolic cost resulting in the significant biomass loss in ANBW4B and ANDW7B, but particularly evident in the former (Table 1). The stronger investment in electron carriers in ANBW4B (Fig. 5f) provides a satisfactory explanation for its growth retardation specifically under FL, which previously remained elusive, given the similar capacity of electron flow control under CL and FL [15]. ANK32A illustrates a paradoxical "side effect" of its impressive investment in electron carriers and, particularly, in PSI end electron acceptors, i.e., the acquisition of a singular resistance to growth under a FL regime. Although the $P700^+$ and I-P phase kinetics clearly indicate a larger bottleneck in electron transport from PQ to end acceptors in ANK32A, the slowed I-P rise in FL plants suggests the occurrence of favourable adjustments similar to the WT line, e.g., not occurring in ANDW7B (Fig. 11c, l).

In conclusion, F_V/F_M and $\Delta V_{IP}/\Delta V_{JP}$ emerge as robust phenotypic indexes, which appear valid across bread and durum wheat, sensitive to the growth light regime, and largely age-independent. The severity of wheat mutants is related to an excessively fast flow of electrons from PQ pool to the end acceptors, as an intrinsic property of the thylakoid membrane. The increase in the pool size of the PSI end electron acceptors can be interpreted as a compensative response to alleviate the PSI acceptor-side limitation and is also favourable to the successful acclimation to a FL regime.

Authors' Contributions

LF, MZ, MB conceived the experiment; MK set up and managed the SPPU facility for the experiment; LF and MK performed the experiment and collected fluorescence data; LF, MK, AC analysed the data; LF, MZ, SP, SIA, MB interpreted the results; LF, MB supervised the research; LF wrote the manuscript, which all authors reviewed and edited.

CRediT authorship contribution statement

Lorenzo Ferroni: Conceptualization, Investigation, Supervision, Formal analysis, Writing – original draft. **Marek Živčak:** Conceptualization, Methodology, Formal analysis, Data curation, Writing – review & editing. **Marek Kovar:** Investigation, Methodology, Formal analysis, Data curation. **Andrea Colpo:** Formal analysis. **Simonetta Pancaldi:** Conceptualization. **Suleyman I. Allakhverdiev:** Supervision. **Marian Brestič:** Conceptualization, Writing – review & editing, Supervision, Funding acquisition, Resources.

Declaration of Competing Interest

The authors declare that there is no competing interest in this work.

Acknowledgments

This work was performed within the European Plant Phenotyping Network 2020 (EPPN^{2020}) and the Slovak Plant Phenotyping Network (SKPPN). In particular, the authors acknowledge the financial support provided by: the Access to Research Infrastructures activity in the Horizon2020 Programme of the EU (EPPN2020 Grant Agreement 731013) for the experiment "TriPUDIUM- TRIticum Photosynthesis Under Drought and fluctuating Irradiance: Use of Mutants phenotyping to approach crop photosynthetic regulation"; the Slovak Plant Phenotyping Network with project EPPN2020-OPVaI-VA - ITMS313011T813 (granted to M.B.); and the University of Ferrara (FAR2019 granted to L. F.). The results (Fig. 8) were obtained within the state assignment of the Ministry of Science and Higher Education of the Russian Federation (project No. 122050400128-1 granted to S.I.A.). The authors are grateful to Professor Nobuyoshi Watanabe (College of Agriculture, Ibaraki University, Japan) for the kind gift of the wheat mutants used in this study.

Appendix A. Supplementary Data

Supplementary data to this article can be found online at https://doi.org/10.1016/j.jphotobiol.2022.112549.

References

[1] J.M. Anderson, W.S. Chow, D.J. Goodchild, Thylakoid membrane organisation in sun/shade acclimation, Funct. Plant Biol. 15 (2) (1988) 11–26, https://doi.org/10.1071/PP9880011.
[2] J.R. Andrews, M.J. Fryer, N.R. Baker, Consequences of LHC II deficiency for photosynthetic regulation in chlorina mutants of barley, Photosynth. Res. 44 (1995) 81–91, https://doi.org/10.1007/BF00018299.
[3] L.W. Bielczynski, G. Schansker, R. Croce, Effect of light acclimation on the organization of photosystem II super- and sub-complexes in *Arabidopsis thaliana*, Front. Plant Sci. 7 (2016) 105, https://doi.org/10.3389/fpls.2016.00105.
[4] L.W. Bielczynski, G. Schansker, R. Croce, Consequences of the reduction of the photosystem II antenna size on the light acclimation capacity of *Arabidopsis thaliana*, Plant Cell Environ. 43 (4) (2020) 866–879, https://doi.org/10.1111/pce.13701.
[5] I.A. Blanco, S. Rajaram, W.E. Kronstad, M.P. Reynolds, Physiological performance of synthetic hexaploid wheat-derived populations, Crop Sci. 40 (5) (2000) 1257–1263, https://doi.org/10.2135/cropsci2000.4051257x.
[6] M. Brestič, M. Živčak, K. Kunderlikova, O. Sytar, H. Shao, H.M. Kalaji, S. I. Allakhverdiev, Low PSI content limits the photoprotection of PSI and PSII in early growth stages of chlorophyll *b*-deficient wheat mutant lines, Photosynth. Res. 125 (1) (2015) 151–166, https://doi.org/10.1007/s11120-015-0093-1.
[7] M. Brestič, M. Živčak, K. Kunderlikova, S.I. Allakhverdiev, High temperature specifically affects the photoprotective responses of chlorophyll *b*-deficient wheat mutant lines, Photosynth. Res. 130 (1) (2016) 251–266, https://doi.org/10.1007/s11120-016-0249-7.
[8] C. Cascio, M. Schaub, K. Novak, R. Desotgiu, F. Bussotti, R.J. Strasser, Foliar responses to ozone of *Fagus sylvatica* L. seedlings grown in shaded and in full sunlight conditions, Environ. Exp. Bot. 68 (2010) 188–197, https://doi.org/10.1016/j.envexpbot.2009.10.003.
[9] M.G. Ceppi, A. Oukarroum, N. Çiçek, R.J. Strasser, G. Schansker, The IP amplitude of the fluorescence rise OJIP is sensitive to changes in the photosystem I content of leaves: a study on plants exposed to magnesium and sulfate deficiencies, drought stress and salt stress, Physiol. Plant. 144 (2012) 277–288, https://doi.org/10.1111/j.1399-3054.2011.01549.x.
[10] E. Chovanček, M. Živčak, M. Brestič, S. Hussain, S.I. Allakhverdiev, The different patterns of post-heat stress responses in wheat genotypes: the role of the transthylakoid proton gradient in efficient recovery of leaf photosynthetic capacity, Photosynth. Res. (2021), https://doi.org/10.1007/s11120-020-00812-0.
[11] B. Demmig-Adams, C.M. Cohu, O. Muller, W.W. Adams, Modulation of photosynthetic energy conversion efficiency in nature: from seconds to seasons, Photosynth. Res. 113 (2012) 75–88, https://doi.org/10.1007/s11120-012-9761-6.
[12] E. Dinç, M.G. Ceppi, S.Z. Tóth, S. Bottka, G. Schansker, The chl *a* fluorescence intensity is remarkably insensitive to changes in the chlorophyll content of the leaf as long as the chl *a*/*b* ratio remains unaffected, Biochim. Biophys. Acta 1817 (2012) 770–779, https://doi.org/10.1016/j.bbabio.2012.02.003.
[13] L.N.M. Duysens, H.E. Sweers, Mechanisms of two photochemical reactions in algae as studied by means of fluorescence, in: Studies on Microalgae and Photosynthetic bacteria, Special Issue of Plant and Cell Physiology, Japanese Society of Plant Physiologists, University of Tokyo Press, Tokyo, 1963, pp. 353–372.
[14] T.G. Falbel, J.B. Meehl, L.A. Staehelin, Severity of mutant phenotype in a series of chlorophyll-deficient wheat mutants depends on light intensity and the severity of the block in chlorophyll synthesis, Plant Physiol. 112 (2) (1996) 821–832, https://doi.org/10.1104/pp.112.2.821.
[15] L. Ferroni, M. Živčak, O. Sytar, M. Kovár, N. Watanabe, S. Pancaldi, C. Baldisserotto, M. Brestič, Chlorophyll-depleted wheat mutants are disturbed in photosynthetic electron flow regulation but can retain an acclimation ability to a fluctuating light regime, Environ. Exp. Bot. 178 (2020), 104156, https://doi.org/10.1016/j.envexpbot.2020.104156.
[16] L. Ferroni, A. Colpo, C. Baldisserotto, S. Pancaldi, In an ancient vascular plant the intermediate relaxing component of NPQ depends on a reduced stroma: evidence from dithiothreitol treatment, J. Photochem. Photobiol. B Biol. 215 (2021), 112114, https://doi.org/10.1016/j.jphotobiol.2020.112114.
[17] R. Furutani, K. Ifuku, Y. Suzuki, K. Noguchi, G. Shimakawa, S. Wada, A. Makino, T. Sohtome, C. Miyake, P700 oxidation suppresses the production of reactive oxygen species in photosystem I, in: T. Hisabori (Ed.), ATP Synthase in Photosynthetic Organisms, Avdances in Botanical Research 96, Elsevier, London, 2020, pp. 151–176, https://doi.org/10.1016/bs.abr.2020.08.001.
[18] B. Genty, J.-M. Briantais, N.R. Baker, The relationship between the quantum yield of photosynthetic electron transport and quenching of chlorophyll fluorescence,

Biochim. Biophys. Acta 990 (1989) 87–92, https://doi.org/10.1016/S0304-4165(89)80016-9.
[19] M.L. Ghirardi, A. Melis, Chlorophyll *b* deficiency in soybean mutants. I. Effects on photosystem stoichiometry and chlorophyll antenna size, Biochim. Biophys. Acta 932 (1986) 130–137, https://doi.org/10.1016/0005-2728(86)90069-1.
[20] Y. Guo, Y. Lu, V. Goltsev, R.J. Strasser, H.M. Kalaji, H. Wang, X. Wang, S. Chen, S. Qiang, Comparative effect of tenuazonic acid, diuron, bentazone, dibromothymoquinone and methyl viologen on the kinetics of Chl *a* fluorescence rise OJIP and the MR_{820} signal, Plant Physiol. Biochem. 156 (2020) 39–48, https://doi.org/10.1016/j.plaphy.2020.08.044.
[21] B. Hsu, Y. Lee, The photosystem II heterogeneity of chlorophyll *b*-deficient mutants of rice: a fluorescence induction study, Austr. J. Plant Physiol. 22 (1995) 195–200, https://doi.org/10.1071/PP9950195.
[22] W. Huang, Y.J. Yang, S.B. Zhang, Photoinhibition of photosystem I under fluctuating light is linked to the insufficient ΔpH upon a sudden transition from low to high light, Environ. Exp. Bot. 160 (2019) 112–119, https://doi.org/10.1016/j.envexpbot.2019.01.012.
[23] W. Huang, Y.J. Yang, S.B. Zhang, The role of water-water cycle in regulating the redox state of photosystem I under fluctuating light, Biochim. Biophys. Acta Bioenerg. 1860 (5) (2019) 383–390, https://doi.org/10.1016/j.bbabio.2019.03.007.
[25] H.M. Kalaji, G. Schansker, R.J. Ladle, et al., Frequently asked questions about chlorophyll fluorescence: practical issues, Photosynth. Res. 122 (2014) 121–158, https://doi.org/10.1007/s11120-014-0024-6.
[26] H.M. Kalaji, A. Jajoo, A. Oukarroum, et al., Chlorophyll *a* fluorescence as a tool to monitor physiological status of plants under abiotic stress conditions, Acta Physiol. Plant. 38 (2016) 102, https://doi.org/10.1007/s11738-016-2113-y.
[27] H.M. Kalaji, G. Schansker, M. Brestič, et al., Frequently asked questions about in vivo chlorophyll fluorescence: the sequel, Photosynth. Res. 132 (2017) 13–66, https://doi.org/10.1007/s11120-016-0318-y.
[28] H. Kirchhoff, W. Haase, S. Haferkamp, T. Schott, M. Borinski, U. Kubitscheck, M. Rögner, Structural and functional self-organization of photosystem II in grana thylakoids, Biochim. Biophys. Acta 1767 (2007) 1180–1188, https://doi.org/10.1016/j.bbabio.2007.05.009.
[29] C. Klughammer, U. Schreiber, An improved method, using saturating light pulses, for the determination of photosystem I quantum yield via $P700^+$-absorbance changes at 830 nm, Planta 192 (1994) 261–268, https://doi.org/10.1007/BF01089043.
[30] M. Kono, I. Terashima, Long-term and short-term responses of the photosynthetic electron transport to fluctuating light, J. Photochem. Photobiol. B Biol. 137 (2014) 89–99, https://doi.org/10.1016/j.jphotobiol.2014.02.016.
[31] S.F. Koval, The catalogue of near-isogenic lines of Novosibirskaya 67 common wheat and principles of their use in experiments, Russ. J. Genet. 33 (1997) 995–1000.
[32] K. Kosuge, N. Watanabe, T. Kuboyama, Comparative genetic mapping of homoeologous genes for the chlorina phenotype in the genus *Triticum*, Euphytica 179 (2) (2011) 257–263, https://doi.org/10.1007/s10681-010-0302-0.
[33] M. Kozuleva, T. Goss, M. Twachtmann, K. Rudi, J. Trapka, J. Selinski, B. Ivanov, P. Garapati, H.J. Steinhoff, et al., Ferredoxin:NADP(H) oxidoreductase abundance and location influences redox poise and stress tolerance, Plant Physiol. 172 (2016) 1480–1493, https://doi.org/10.1104/pp.16.01084.
[34] A. Laisk, V. Oja, Kinetics of photosystem II electron transport: a mathematical analysis based on chlorophyll fluorescence induction, Photosynth. Res. 136 (1) (2018) 63–82, https://doi.org/10.1007/s11120-017-0439-y.
[35] A.D.B. Leakey, M.C. Press, J.D. Scholes, J.R. Watling, Relative enhancement of photosynthesis and growth at elevated CO_2 is greater under sunflecks than uniform irradiance in a tropical rain forest tree seedling, Plant Cell Environ. 25 (2002) 1701–1714, https://doi.org/10.1046/j.1365-3040.2002.00944.x.
[36] Y.T. Li, C. Yang, Z.S. Zhang, S.J. Zhao, H.Y. Gao, Photosynthetic acclimation strategies in response to intermittent exposure to high light intensity in wheat (*Triticum aestivum* L.), Environ. Exp. Bot. 181 (2021) 104275, https://doi.org/10.1016/j.envexpbot.2020.104275.
[37] N. Li, J. Jia, C. Xia, X. Liu, X. Kong, Characterization and mapping of novel chlorophyll deficient mutant genes in durum wheat, Breed. Sci. 63 (2) (2013) 169–175, https://doi.org/10.1270/jsbbs.63.169.
[38] H.L. Lichtenthaler, Chlorophyll and carotenoids: pigments of photosynthetic biomembranes, Methods Enzymol. 148 (1987) 350–382.
[39] M. Lintala, N. Lehtimaki, J.P. Benz, A. Jungfer, J. Soll, E.M. Aro, B. Bolter, P. Mulo, Depletion of leaf- type ferredoxin-$NADP^+$ oxidoreductase results in the permanent induction of photoprotective mechanisms in Arabidopsis chloroplasts, Plant J. 70 (2012) 809–817, https://doi.org/10.1111/j.1365-313X.2012.04930.x.
[40] A. Malnoë, Photoinhibition or photoprotection of photosynthesis? Update on the (newly termed) sustained quenching component qH, Environ. Exp. Bot. 154 (2018) 123–133, https://doi.org/10.1016/j.envexpbot.2018.05.005.
[41] L.A. Malone, M.S. Proctor, A. Hitchcock, C.N. Hunter, M.P. Johnson, Cytochrome b_6f –orchestrator of photosynthetic electron transfer, Biochim. Biophys. Acta Bioenerg. 148380 (2021), https://doi.org/10.1016/j.bbabio.2021.148380.
[42] H. Mao, M. Chen, Y. Su, N. Wu, M. Yuan, S. Yuan, M. Brestič, M. Živčak, H. Zhang, Y. Chen, Comparison on photosynthesis and antioxidant defense systems in wheat with different ploidy levels and octoploid triticale, Int. J. Mol. Sci. 19 (10) (2018) 3006, https://doi.org/10.3390/ijms1 91030 06.
[43] J.C. Munday Jr., Govindjee, Light-induced changes in the fluorescence yield of chlorophyll *a* in vivo: III. The dip and the peak in the fluorescence transient of *Chlorella pyrenoidosa*, Biophys. J. 9 (1969) 1–21, https://doi.org/10.1016/S0006-3495(69)86365-4.
[44] Y. Munekage, M. Hojo, J. Meurer, T. Endo, M. Tasaka, T. Shikanai, PGR5 is involved in cyclic electron flow around photosystem I and is essential for photoprotection in Arabidopsis, Cell 110 (2002) 361–371, https://doi.org/10.1016/s0092-8674(02)00867-x.
[45] S. Mathur, S.I. Allakhverdiev, A. Jajoo, Analysis of high temperature stress on the dynamics of antenna size and reducing side heterogeneity of photosystem II in wheat leaves (*Triticum aestivum*), Biochim. Biophys. Acta 1807 (2011) 22–29, https://doi.org/10.1016/j.bbabio.2010.09.001.
[46] S. Mathur, L. Jain, A. Jajoo, Photosynthetic efficiency in sun and shade plants, Photosynthetica 56 (1) (2018) 354–365, https://doi.org/10.1007/s11099-018-0767-y.
[47] A. Morales, E. Kaiser, Photosynthetic acclimation to fluctuating irradiance in plants, Front. Plant Sci. 11 (2020) 268, https://doi.org/10.3389/fpls.2020.00268.
[48] L. Nicol, W.J. Nawrocki, R. Croce, Disentangling the sites of non-photochemical quenching in vascular plants, Nat. Plants 5 (2019) 1177–1183, https://doi.org/10.1038/s41477-019-0526-5.
[49] S. Niedermaier, T. Schneider, M.O. Bahl, S. Matsubara, P.F. Huesgen, Photoprotective acclimation of the *Arabidopsis thaliana* leaf proteome to fluctuating light, Front. Genet. 11 (2020) 154, https://doi.org/10.3389/fgene.2020.00154.
[50] A. Oukarroum, G. Schanske, R.J. Strasser, Drought stress effects on photosystem I content and photosystem II thermotolerance analyzed using Chl *a* fluorescence kinetics in barley varieties differing in their drought tolerance, Physiol. Plant. 137 (2009) 188–199, https://doi.org/10.1111/j.1399-3054.2009.01273.x.
[51] J.F. Palatnik, V.B. Tognetti, H.O. Poli, R.E. Rodriguez, N. Blanco, M. Gattuso, M. R. Hajirezaei, U. Sonnewald, E.M. Valle, N. Carrillo, Transgenic tobacco plants expressing antisense ferredoxin-NADP(H) reductase transcripts display increased susceptibility to photo-oxidative damage, Plant J. 35 (2003) 332–341, https://doi.org/10.1046/j.1365-313x.2003.01809.x.
[52] E. Pfündel, Estimating the contribution of photosystem I to total leaf chlorophyll fluorescence, Photosynth. Res. 56 (1998) 185–195, https://doi.org/10.1023/A:1006032804606.
[54] M. Pollastrini, E. Salvatori, L. Fusaro, F. Manes, R. Marzuoli, G. Gerosa, W. Brüggemann, R.J. Strasser, F. Bussotti, Selection of tree species for forests under climate change: is PSI functioning a better predictor for net photosynthesis and growth than PSII? Tree Physiol. 40 (2020) 1561–1571, https://doi.org/10.1093/treephys/tpaa084.
[55] M.Y. Qiao, Y.J. Zhang, L.A. Liu, L. Shi, Q.H. Ma, W.S. Chow, C.D. Jiang, Do rapid photosynthetic responses protect maize leaves against photoinhibition under fluctuating light? Photosynth. Res. (2020) https://doi.org/10.1007/s11120-020-00780-5.
[56] R.E. Rodriguez, A. Lodeyro, H.O. Poli, M. Zurbriggen, M. Peisker, J.F. Palatnik, V. B. Tognetti, H. Tschiersch, M.R. Hajirezaei, E.M. Valle, et al., Transgenic tobacco plants overexpressing chloroplastic ferredoxin-NADP(H) reductase display normal rates of photosynthesis and increased tolerance to oxidative stress, Plant Physiol. 143 (2007) 639–649, https://doi.org/10.1104/pp.106.090449.
[57] M. Rodriguez-Heredia, F. Saccon, S. Wilson, G. Finazzi, A.V. Ruban, G.T. Hanke, Protection of photosystem I during sudden light stress depends on ferredoxin:NADP(H) reductase abundance and interactions, Plant Physiol. 188 (2022) 1028–1042, https://doi.org/10.1093/plphys/kiab550.
[58] G. Schansker, A. Srivastava, R.J. Strasser, Characterization of the 820-nm transmission signal paralleling the chlorophyll a fluorescence rise (OJIP) in pea leaves, Funct. Plant Biol. 30 (2003) 785–796, https://doi.org/10.1071/FP03032.
[59] G. Schansker, S.Z. Tóth, R.J. Strasser, Methylviologen and dibromothymoquinone treatments of pea leaves reveal the role of photosystem I in the Chl *a* fluorescence rise OJIP, Biochim. Biophys. Acta 1706 (2005) 250–261, https://doi.org/10.1016/j.bbabio.2004.11.006.
[60] G. Schansker, S.Z. Tóth, R.J. Strasser, Dark-recovery of the Chl *a* fluorescence transient (OJIP) after light adaptation: the qT component of non-photochemical quenching is related to an activated photosystem I acceptor side, Biochim. Biophys. Acta 1757 (2006) 787–797, https://doi.org/10.1016/j.bbabio.2006.04.019.
[61] G. Schansker, S.Z. Tóth, L. Kovács, A.R. Holzwarth, G. Garab, Evidence for a fluorescence yield change driven by a light induced conformational change within photosystem II during the fast chlorophyll *a* fluorescence rise, Biochim. Biophys. Acta 1807 (2011) 1032–1043, https://doi.org/10.1016/j.bbabio.2011.05.022.
[62] G. Schansker, S.Z. Tóth, A.R. Holzwarth, G. Garab, Chlorophyll *a* fluorescence: beyond the limit of the Q_A model, Photosynth. Res. 120 (2014) 43–58, https://doi.org/10.1007/s11120-013-9806-5.
[63] T. Schneider, A. Bolger, J. Zeier, S. Preiskowski, V. Benes, S. Trenkamp, B. Usadel, E.M. Farré, S. Matsubara, Fluctuating light interacts with time of day and leaf development stage to reprogram gene expression, Plant Physiol. 179 (2019) 1632–1657, https://doi.org/10.1104/pp.18.01443.
[64] U. Schreiber, K. Klughammer, Evidence for variable chlorophyll fluorescence of photosystem I in vivo, Photosynth. Res. 149 (2021) 213–231, https://doi.org/10.1007/s11120-020-00814-y.
[65] G. Shimakawa, C. Miyake, Oxidation of P700 ensures robust photosynthesis, Front. Plant Sci. 9 (2018) 1617, https://doi.org/10.3389/fpls.2018.01617.
[66] G. Shimakawa, C. Miyake, What quantity of photosystem I is optimum for safe photosynthesis? Plant Physiol. 179 (4) (2019) 1479–1485, https://doi.org/10.1104/pp.18.01493.
[67] T. Schumann, S. Paul, M. Melzer, P. Dörmann, P. Jahns, Plant growth under natural light conditions provides highly flexible short-term acclimation properties toward high light stress, Front. Plant Sci. 8 (2017) 681, https://doi.org/10.3389/fpls.2017.00681.
[68] G. Sipka, M. Magyar, A. Mezzetti, P. Akhtar, Q. Zhu, Y. Xiao, G. Han, S. Santabarbara, J.-R. Shen, P.H. Lambrev, G. Garab, Light-adapted charge-separated state of photosystem II: structural and functional dynamics of the closed

reaction center, Plant Cell 33 (2021) 1286–1302, https://doi.org/10.1093/plcell/koab008.
[69] R.A. Slattery, B.J. Walker, A.P.M. Weber, D.R. Ort, The impacts of fluctuating light on crop performance, Plant Physiol. 176 (2018) 990–1003, https://doi.org/10.1104/pp.17.01234.
[70] A. Stirbet, Govindjee, On the relation between the Kautsky effect (chlorophyll *a* fluorescence induction) and photosystem II: basics and applications of the OJIP fluorescence transient, J. Photochem. Photobiol. B 104 (2011) 236–257, https://doi.org/10.1016/j.jphotobiol.2010.12.010.
[71] A. Stirbet, Govindjee, Chlorophyll a fluorescence induction: a personal perspective of the thermal phase, the J–I–P rise, Photosynth. Res. 113 (2012) 15–61, https://doi.org/10.1007/s11120-012-9754-5.
[72] A. Stirbet, D. Lazár, J. Kromdijk, Govindjee, Chlorophyll a fluorescence induction: can just a one-second measurement be used to quantify abiotic stress responses? Photosynthetica 56 (2018) 86–104, https://doi.org/10.1007/s11099-018-0770-3.
[73] R.J. Strasser, M. Tsimilli-Michael, A. Srivastava, Analysis of the chlorophyll *a* fluorescence transient, in: G. Papageorgiou, Govindjee (Eds.), Chlorophyll *a* Fluorescence: A Signature of Photosynthesis, Advances in Photosynthesis and Respiration, Springer, Dordrecht, 2004, pp. 321–362.
[74] H. Sun, Y.-J. Yang, W. Huang, The water-water cycle is more effective in regulating redox state of photosystem I under fluctuating light than cyclic electron transport, Biochim. Biophys. Acta Bioenerg. 1861 (9) (2020), 148235, https://doi.org/10.1016/j.bbabio.2020.148235.
[75] H. Sun, S.B. Zhang, T. Liu, W. Huang, Decreased photosystem II activity facilitates acclimation to fluctuating light in the understory plant *Paris polyphylla*, Biochim. Biophys. Acta Bioenerg. 1861 (2) (2020), 148135, https://doi.org/10.1016/j.bbabio.2019.148135.
[76] M. Suorsa, S. Järvi, M. Grieco, M. Nurmi, M. Pietrzykowska, M. Rantala, S. Kangasjärvi, V. Paakkarinen, M. Tikkanen, S. Jansson, E.M. Aro, PROTON GRADIENT REGULATION5 is essential for proper acclimation of *Arabidopsis* photosystem I to naturally and artificially fluctuating light conditions, Plant Cell 24 (7) (2012) 2934–2948, https://doi.org/10.1105/tpc.112.097162.
[77] Y. Tanaka, S. Adachi, W. Yamori, Natural genetic variation of the photosynthetic induction response to fluctuating light environment, Curr. Opin. Plant Biol. 49 (2019) 52–59, https://doi.org/10.1016/j.pbi.2019.04.010.
[78] T. Terao, S. Katoh, Antenna sizes of photosystem I and photosystem II in chlorophyll *b*-deficient mutants of rice. Evidence for an antenna function of photosystem II centers that are inactive in electron transport, Plant Cell Physiol. 37 (1996) 307–312, https://doi.org/10.1093/oxfordjournals.pcp.a028947.
[79] T. Terao, K. Sonoike, J.Y. Yamazaki, Y. Kamimura, S. Katoh, Stoichiometries of photosystem I and photosystem II in rice mutants differently deficient in chlorophyll *b*, Plant Cell Physiol. 37 (1996) 299–306, https://doi.org/10.1093/oxfordjournals.pcp.a028946.
[80] I. Terashima, M. Matsuo, Y. Suzuki, W. Yamori, M. Kono, Photosystem I in low light-grown leaves of *Alocasia odora*, a shade-tolerant plant, is resistant to fluctuating light-induced photoinhibition, Photosynth. Res. (2021), https://doi.org/10.1007/s11120-021-00832-4.
[81] M. Tikkanen, M. Grieco, M. Nurmi, M. Rantala, M. Suorsa, E.M. Aro, Regulation of the photosynthetic apparatus under fluctuating growth light, Phil Trans Royal Soc B: Biol Sci 367 (1608) (2012) 3486–3493, https://doi.org/10.1098/rstb.2012.0067.
[83] M. Tsimilli-Michael, R. Strasser, In vivo assessment of plants' vitality: Applications in detecting and evaluating the impact of mycorrhization on host plants, in: A. Varma (Ed.), Mycorrhiza: State of the Art, Genetics and Molecular Biology, Eco-Function, Biotechnology, Eco-Physiology, Structure and Systematics, 3rd ed., Springer, Dordrecht, 2008, pp. 679–703.
[84] M. Tsimilli-Michael, Revisiting JIP-test: An educative review on concepts, assumptions, approximations, definitions and terminology, Photosynthetica 58 (2020) 275–292, https://doi.org/10.32615/ps.2019.150.
[85] S.Z. Tóth, G. Schansker, R.J. Strasser, A non-invasive assay of the plastoquinone pool redox state based on the OJIP-transient, Photosynth. Res. 93 (2007) 193–203, https://doi.org/10.1007/s11120-007-9179-8.
[86] W. Vredenberg, Kinetic analyses and mathematical modeling of primary photochemical and photoelectrochemical processes in plant photosystems, Biosystems 103 (2) (2011) 138–151, https://doi.org/10.1016/j.biosystems.2010.10.016.
[87] H. Yamamoto, T. Shikanai, PGR5-dependent cyclic electron flow protects photosystem I under fluctuating light at donor and acceptor sides, Plant Physiol. 179 (2) (2019) 588–600, https://doi.org/10.1104/pp.18.01343.
[88] W. Yamori, Photosynthetic response to fluctuating environments and photoprotective strategies under abiotic stress, J. Plant Res. 129 (3) (2016) 379–395, https://doi.org/10.1007/s10265-016-0816-1.
[89] N. Watanabe, S. Kobayashi, Y. Furuta, Effect of genome and ploidy on photosynthesis of wheat, Euphytica 94 (3) (1997) 303–309, https://doi.org/10.1023/a:1002936019332.
[90] N. Watanabe, S.F. Koval, Mapping of chlorina mutant genes on the long arm of homoeologous group 7 chromosomes in common wheat with partial deletion lines, Euphytica 129 (2003) 259–265, https://doi.org/10.1023/A:1022276724354.
[92] H. Wu, N. Shi, X. An, C. Liu, H. Fu, L. Cao, Y. Feng, D. Sun, L. Zhang, Candidate genes for yellow leaf color in common wheat (*Triticum aestivum* L.) and major related metabolic pathways according to transcriptome profiling, Int. J. Mol. Sci. 19 (6) (2018) 1594, https://doi.org/10.3390/ijms19061594.
[93] Y. Wang, W. Zheng, W. Zheng, J. Zhu, Z. Liu, J. Qin, H. Li, Physiological and transcriptomic analyses of a yellow-green mutant with high photosynthetic efficiency in wheat (*Triticum aestivum* L.), Funct. Integr. Genomics 18 (2017) 175–194, https://doi.org/10.1007/s10142-017-0583-7.
[94] G. Wang, F. Zeng, P. Song, P. Sun, Q. Wang, J. Wang, Effects of reduced chlorophyll content on photosystem functions and photosynthetic electron transport rate in rice leaves, J. Plant Physiol. 272 (2022), 153669, https://doi.org/10.1016/j.jplph.2022.153669.
[95] M. Živčak, M. Brestič, H.M. Kalaji, Govindjee, Photosynthetic responses of sun- and shade-grown barley leaves to high light: is the lower PSII connectivity in shade leaves associated with protection against excess of light? Photosynth. Res. 119 (2014) 339–354, https://doi.org/10.1007/s11120-014-9969-8.
[96] M. Živčak, H.M. Kalaji, H.B. Shao, K. Olšovská, M. Brestič, Photosynthetic proton and electron transport in wheat leaves under prolonged moderate drought stress, J. Photochem. Photobiol. B 137 (2014) 107–115, https://doi.org/10.1016/j.jphotobiol.2014.01.007.
[97] M. Živčak, M. Brestič, K. Kunderlikova, K. Olšovská, S.I. Allakhverdiev, Effect of photosystem I inactivation on chlorophyll *a* fluorescence induction in wheat leaves: does activity of photosystem I play any role in OJIP rise? J. Photochem. Photobiol. B Biol. 152 (2015) 318–324, https://doi.org/10.1016/j.jphotobiol.2015.08.024.
[98] M. Živčak, M. Brestič, L. Botyanszka, Y.E. Chen, S.I. Allakhverdiev, Phenotyping of isogenic chlorophyll-less bread and durum wheat mutant lines in relation to photoprotection and photosynthetic capacity, Photosynth. Res. 139 (1) (2019) 239–251, https://doi.org/10.1007/s11120-018-0559-z.